



ALMA MATER STUDIORUM  
UNIVERSITÀ DI BOLOGNA

## ARCHIVIO ISTITUZIONALE DELLA RICERCA

### Alma Mater Studiorum Università di Bologna Archivio istituzionale della ricerca

Developing effective subsoil reference model for seismic microzonation studies: Central Italy case studies

This is the final peer-reviewed author's accepted manuscript (postprint) of the following publication:

*Published Version:*

Pierluigi Pieruccini, Enrico Paolucci, Pier Lorenzo Fantozzi, Duccio Naldini, Dario Albarello (2022).  
Developing effective subsoil reference model for seismic microzonation studies: Central Italy case studies.  
NATURAL HAZARDS, 112(1), 451-474 [10.1007/s11069-021-05188-5].

*Availability:*

This version is available at: <https://hdl.handle.net/11585/950505> since: 2023-12-12

*Published:*

DOI: <http://doi.org/10.1007/s11069-021-05188-5>

*Terms of use:*

Some rights reserved. The terms and conditions for the reuse of this version of the manuscript are specified in the publishing policy. For all terms of use and more information see the publisher's website.

This item was downloaded from IRIS Università di Bologna (<https://cris.unibo.it/>).  
When citing, please refer to the published version.

(Article begins on next page)

This is the final peer-reviewed accepted manuscript of:

Pieruccini, P., Paolucci, E., Fantozzi, P.L. et al. Developing effective subsoil reference model for seismic microzonation studies: Central Italy case studies. *Nat Hazards* 112, 451–474 (2022).

The final published version is available online at: <https://doi.org/10.1007/s11069-021-05188-5>

#### Terms of use:

Some rights reserved. The terms and conditions for the reuse of this version of the manuscript are specified in the publishing policy. For all terms of use and more information see the publisher's website.

*This item was downloaded from IRIS Università di Bologna (<https://cris.unibo.it/>)*

***When citing, please refer to the published version.***

# 1 DEVELOPING EFFECTIVE SUBSOIL REFERENCE MODEL FOR SEISMIC 2 MICROZONATION STUDIES: CENTRAL ITALY CASE STUDIES

3 Pierluigi Pieruccini<sup>1</sup>, Enrico Paolucci<sup>2</sup>, Pier Lorenzo Fantozzi<sup>2</sup>, Duccio Naldini<sup>2</sup>, Dario Albarello<sup>2,3</sup>

4 <sup>1</sup>Dipartimento di Scienze della Terra, Università degli Studi di Torino, Via Valperga Caluso 35, 10125 Turin, Italy

5 <sup>2</sup>Dipartimento di Scienze Fisiche, della Terra e dell'Ambiente, Università degli Studi di Siena, Via Laterina 8, 53100  
6 Siena, Italy

7 <sup>3</sup>Istituto di Geologia Ambientale e Geoingegneria (IGAG), Consiglio Nazionale delle Ricerche (CNR), Area della Ricerca  
8 di Roma 1, Montelibretti, Italy

9 Corresponding Author: Dario Albarello

10 E-mail address: [dario.albarello@unisi.it](mailto:dario.albarello@unisi.it)

11 Keywords: Seismic Microzonation, Engineering-Geological Model, site effects, Amplification Factors

## 12 Abstract

13 A general methodological approach is here discussed to integrate geological and geophysical  
14 information in seismic microzonation studies. In particular, the methodology aims at maximizing the  
15 exploitation of low-cost data for extensive preliminary assessment of ground motion amplification  
16 phenomena induced by the local seismostratigraphical configuration. Three main steps are delineated:  
17 a) the combination of geological/geomorphological analyses to develop an Engineering-Geological  
18 Model of the study area; b) targeted geophysical prospecting to provide an Engineering-  
19 Geological/Geophysical Model; c) evaluating effectiveness of Engineering-Geological/Geophysical  
20 Model by estimating expected ground motion amplification phenomena by the use of suitable  
21 computational tools. The workflow is illustrated by a case-study based on a set of villages in the  
22 Umbro-Marchean Apennine (Central Italy) damaged during the Seismic sequence occurred in Central  
23 Italy during 2016-2017.

## 24 1. INTRODUCTION

25 Since the pioneering studies by Baratta (1910) after 1908 Messina Earthquake the significant role of  
26 the local geological-geomorphological setting in controlling the distribution of damages induced by  
27 the seismic ground motion became an important issue later formalized by Medvedev (1965) for  
28 seismic hazard assessment at local scale (Faccioli, 1986). More recently, theoretical modeling and  
29 experimental data put in evidence that the relationships between ground shaking and geological-  
30 geomorphological settings relies on the presence and geometry of sharp variations in the elastic  
31 properties of rocks (seismic impedance contrasts) and associated shear waves velocity ( $V_s$ ) variations  
32 are responsible for seismic energy trapping and resonance phenomena in the shallowest part of the  
33 subsurface and relative interference phenomena of engineering interest (e.g., Kramer, 1996).

34 The most recent seismic codes (e.g., BSSC NHERP, 2000; EN 1998-1, 2004) implement this view to  
35 account for possible ground motion amplification phenomena in the anti-seismic design of new  
36 structures. These codes (and analogous normative documents in national contexts) implicitly  
37 distinguish between the seismic hazard assessment at regional scale (the 'reference' seismic hazard)  
38 and at 'local' level: the first is assessed by considering seismogenic processes and regional scale  
39 radiation pattern of earthquakes, the second by accounting for modification induced on the ground  
40 shacking at small scale (tens to hundreds of meters) geological-geomorphological settings.

41 These modifications are generally estimated by numerical modelling which accounts for the  
42 seismostratigraphical and geotechnical configuration of the local subsoil (e.g., Kramer, 1996). A key

43 element of this procedure is the definition of reference soil condition ('seismic' or 'engineering'  
44 bedrock), where the input seismic motion considered in the modelling is assumed to be known (e.g.,  
45 by regional scale seismic hazard assessment). The parameterization of these models (in terms of Vs  
46 profiles, rigidity reduction and damping decay curves) must be performed by borehole and/or surface  
47 geophysical measurements (mainly active and passive seismic prospecting, e.g., Foti et al., 2011;  
48 Caielli et al., 2020) and laboratory tests (as concerns nonlinear aspects of soil dynamics).

49 When single buildings are of concern, seismic characterization relates to relatively small portions of  
50 the subsoil (the so called 'seismic response studies') and the relevant expenses could be supported by  
51 the stakeholders. However, when dealing with areal estimates, this analysis must be performed at  
52 many sites, and this makes the study very expensive, and this may hamper a generalized application  
53 of such analyses where public funds actually available are relatively scarce.

54 To face this problem, the strategies developed under the denomination of "Seismic Microzonation"  
55 (SM) are devoted to seismic hazard assessment at the scale of settlement and surrounding land  
56 (typically municipality). SM requires a strongly multidisciplinary approach must be developed which  
57 takes advantage of a full interoperability between geological/geomorphological surveys, geophysical  
58 prospecting, numerical modelling, and geotechnical laboratory testing. This marked  
59 interdisciplinarity requires a coherent methodological workflow between geologists, geophysicists,  
60 geotechnical engineers and, ultimately, land planners.

61 In the last years, the Italian scientific community (coordinated within the Centre for Seismic  
62 Microzonation and Applications – <https://www.centromicrozonazioneismica.it/en/> under the  
63 coordination of the Civil Protection Department) developed specific guidelines for SM studies  
64 (WSGM 2008; WGSMLA 2010; Various Authors 2011). The guidelines delineate a gradual approach  
65 by defining three levels of SM studies, each characterized by increasing engagement and costs (e.g.,  
66 Albarello, 2017; Moscatelli et al., 2020) in front of improved resolution and completeness. The first  
67 level is basically a collection of available information concerning shallow subsurface (i.e., borehole-  
68 data, geological/geomorphological surveys, geotechnical data) (CTMS, 2018) to assess a Geological-  
69 Geomorphological model after reclassification of geological units into engineering geological units  
70 following their geotechnical properties (thereafter *gt\_units*) (ASTM, 2017; Amanti et al., 2020). This  
71 model subdivides the study area in homogeneous parcels of land (Seismically Homogenous  
72 Microzones, SHM) each characterized by similar expected co-seismic phenomena. Despite of the  
73 inherently semi-qualitative character of the SM first level, its outcomes are of primary importance for  
74 the subsequent levels. In the second level SM, amplification effects induced by the local 1D  
75 stratigraphical configuration are quantified by adopting a simplified approach based on the use of  
76 suitable abacuses (Peruzzi et al., 2016; Albarello et al., 2017; Paolucci et al., 2020). This second level  
77 SM can be seen as the first operative basis for land and emergency planning, providing specific  
78 indications to local authorities as concerns management of preventive activities (e.g., Mori et al.,  
79 2020). The third level SM only concerns small areas where complex effects (induced landslides,  
80 liquefaction, etc.) are expected and where simplified approaches cannot be effectively applied (Caielli  
81 et al., 2020; Ciancimino et al., 2020; Pagliaroli et al., 2020).

82 In this paper, we propose an integrated methodological workflow for SM studies that highlights the  
83 importance and the effectiveness of a complex Engineering Geological Model as basic prerequisite  
84 for 1D modelling of amplification effects. Three main steps are delineated: a) the combination of  
85 geological/geomorphological analyses to develop an Engineering-Geological Model of the study area  
86 (EGM); b) an upgraded model (Engineering-Geological/Geophysical Model, EGGM) by considering  
87 data provided by geophysical targeted prospecting; c) the definition of a SHM map based on EGGM  
88 by the use of suitable computational tools and the evaluation of the coherence of 1D Amplification  
89 Factors against the complexity of the EGGM. The workflow is illustrated by a case study based on a

90 number of villages in Central Italy damaged during a Seismic sequence occurred in Central Italy  
91 during 2016-17 and where an intense SM campaign was carried out to support reconstruction  
92 activities (Moscatelli et al., 2020).

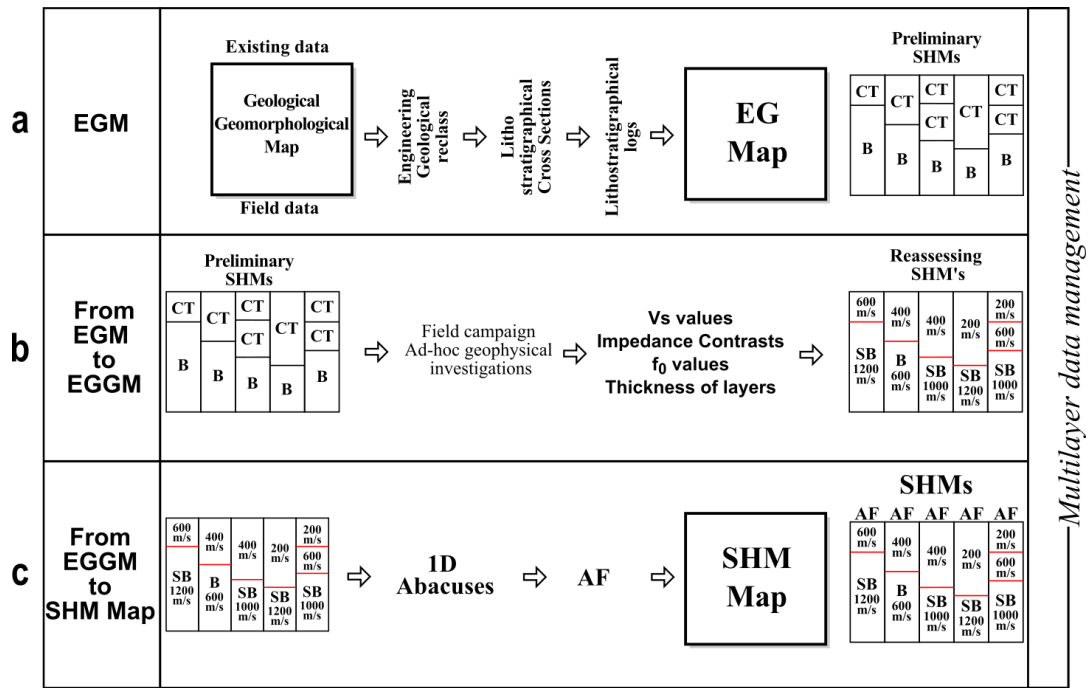
## 93 2. METHODOLOGICAL OUTLINE

94 The proposed methodological workflow is based upon the following steps:

- 95 a) assessment of the Engineering-Geological Model (EGM, Fig. 1a): concerns the definition of the  
96 zones characterised by homogeneous lithostratigraphical and geomorphological settings, including  
97 the semi-quantitative definition of representative lithostratigraphical logs and their geometrical  
98 relationships; in this evaluation the definition of the thickness ranges of the lithostratigraphical layers  
99 is relevant for geometrical relationships. Moreover, the geological units are reclassified in terms of  
100 (gt\_units), *sensu* ASTM (2017) and CTMS (2018);  
101 b) from EGM to the Engineering-Geological/Geophysical Model (EGGM, Fig. 1b): on the basis of  
102 the EGM, quick and low-cost surface geophysical investigations are planned to better constrain the  
103 vertical and lateral stratigraphical setting of SHMs and provide lithostratigraphical layers with  
104 seismic parameters (mainly Vs) and define representative lithostratigraphical logs for each SHM;  
105 c) from EGGM to SHM Map (Fig. 1c): the EGGM is used to attribute Amplification Factor (AF)  
106 values to each SHM. Amplification factors are expressed in the form  
107

$$108 \quad AF_{T_1-T_2} = \frac{\int_{T_1}^{T_2} Sa_0 dT}{\int_{T_1}^{T_2} Sa_i dT} \quad ,[1]$$

109 where  $Sa_i$  e  $Sa_0$  are the acceleration response spectra at the reference soil configuration and at the  
110 surface respectively.  $T_1$  and  $T_2$  are the extrema of range of building resonance periods of concern. In  
111 the Italian practice, three ranges are considered (0.1-0.5 s, 0.4-0.8 s, 0.7-1.1 s) representative of small,  
112 intermediate, and tall buildings (or seismically isolated) buildings. The respective values are  
113 determined from a small set of experimental proxies by using specific seismic abacuses representative  
114 of 1D resonance phenomena (WSGM, 2008). Eventually, presence of significantly different  
115 Amplification Factors within the same SHM may suggest its further subdivision by identifying new  
116 SHMs. The results are shown in a Map.



117

118 Fig. 1. Scheme of the methodological workflow. EGM, Engineering-Geological Model; EG Map, Engineering-Geological  
 119 Map; CT, Cover Terrains; B, Bedrock; EGGM, Engineering-Geological/Geophysical Model; SB, Seismic Bedrock; SHM,  
 120 Seismically Homogenous Microzone; AF, Amplification Factor (eq. 1); red lines within the SHM lithostratigraphical logs  
 121 represent the position of the seismic impedance contrasts.

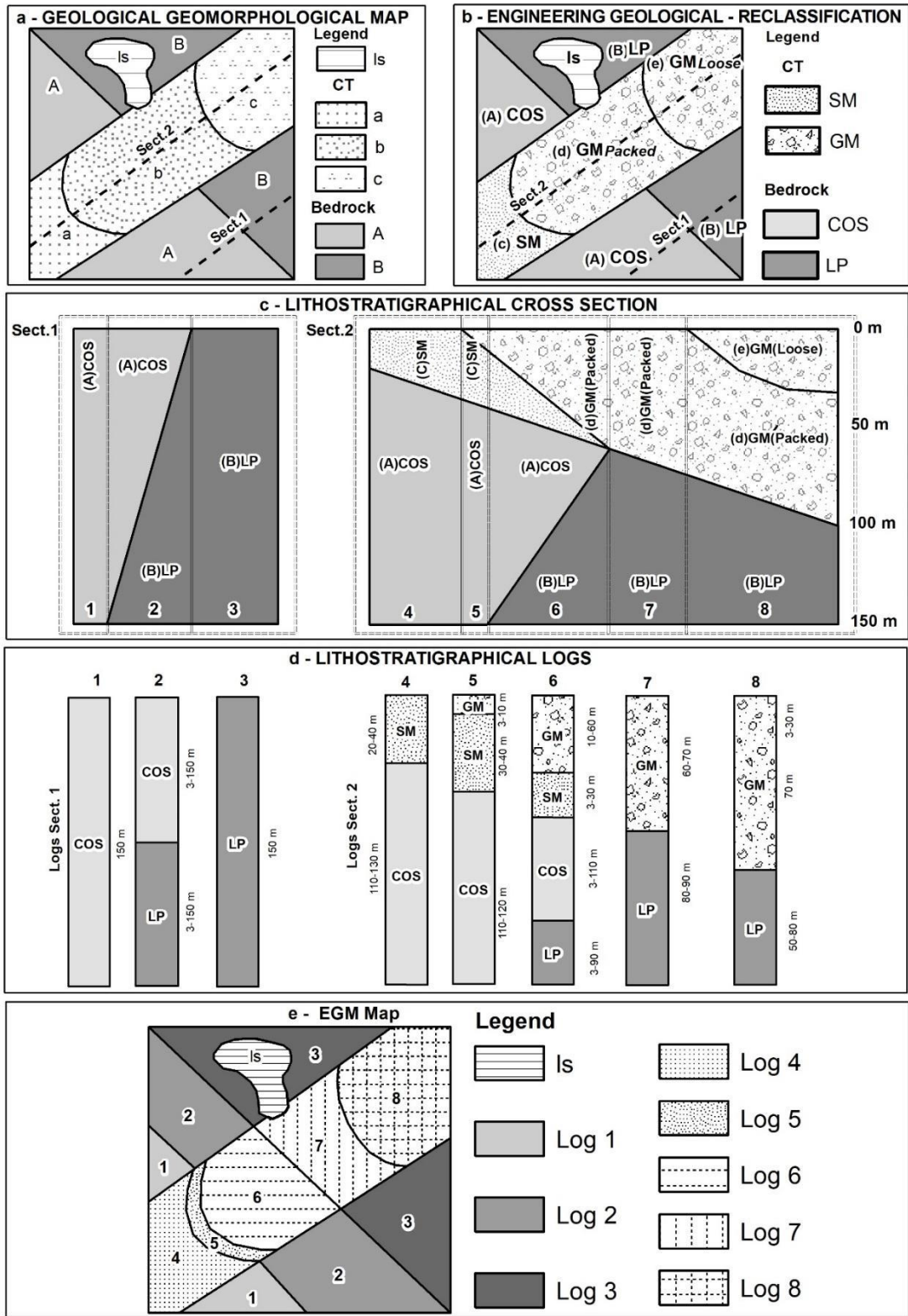
122 **2.1 Assessment of EGM**

123 EGM is a three-dimensional reconstruction of the lithostratigraphical sequences reclassified as  
 124 gt\_units and their volumetric distribution, including unstable areas (gravity phenomena, surface  
 125 faulting, liquefaction and differential soil failures). EGM is represented by a map made of polygons  
 126 classified as Bedrock and Cover Terrains (CT). Bedrock can be defined as the outcropping complex  
 127 geological units/formations (sedimentary, magmatic, metamorphic) or unconformably buried under  
 128 CTs. The last are made by units/formations related to the modelling of the present-day landscape and  
 129 relative surface processes. In the geological-geomorphological setting of the Italian peninsula CTs  
 130 are usually of Quaternary age whereas Bedrock is pre-Quaternary. CT are usually complex  
 131 sedimentary bodies associated to morphogenetic processes (running water, gravity, karst, weathering,  
 132 ice etc.) and therefore with extremely variable lateral extension and thickness. This variability is due  
 133 to the presence of buried morphologies carved on Bedrock and to frequent and abrupt changes of  
 134 facies associated to the different sedimentary environments and therefore showing a strong variability  
 135 of geotechnical/geophysical properties. In terms of seismic behaviour, the sharper impedance contrast  
 136 responsible for the main possible resonance phenomena is expected at the boundary between CTs and  
 137 Bedrock, the latter represented by more rigid material. The high CT thickness variability can therefore  
 138 cause the presence of impedance contrasts located at significantly different depths over distances of  
 139 the order of hundreds of meters: it follows that, in the context of small-scale seismic hazard  
 140 assessment, detailed geological and surveys are mandatory. In this framework, we assumed that  
 141 thickness of the geological bodies in the EGM can be roughly classified as thin (3-10m), intermediate  
 142 (10-100m) and thick (>100m).

143 EGM is at the base of any small-scale seismic hazard investigation and can be assessed only by  
 144 expert-based observations, analysis and synthesis of existing data integrated with field data of new  
 145 acquisitions. Existing data should be filtered according to their importance for EGM definition, such  
 146 as local lithostratigraphical and structural settings, number and thickness of geological layers,

147 geomorphological features and processes and, where available, geophysical and geotechnical  
148 parameters. Such data are usually gathered from National and Local databases and can consists of  
149 geological and geomorphological maps, local investigations such as cores, seismic surveys etc. The  
150 analysis of existing data is crucial to plan any further investigation.

151 In this first step, new field data are usually acquired by means of ex-novo geological and  
152 geomorphological surveys aimed at a more accurate definition of Bedrock and CT. To this purpose,  
153 the adopted legends should be based mainly on lithostratigraphical and morphogenetical criteria.  
154 Existing data and new field data integration lead to the first output that is a traditional Geological-  
155 Geomorphological Map reclassified and translated into an Engineering-Geological Map (Fig. 2a,b).  
156 The dimension of the subsurface volume to be assessed for EGM depends on the wavelength of  
157 seismic waves responsible for the damage of the structures. By assuming that these shear waves  
158 velocities in the shallow subsoil these are in the order of 200-600 m/s, for most common buildings  
159 with natural period of the order of 1s or less (IAEA, 2016) the wavelengths of the order of tens to  
160 hundreds of meters are of main importance. Therefore, the depth of subsoil to be characterized can  
161 be assumed at 150m for most of the situations. By the modelling of lithostratigraphical cross-sections  
162 (Fig. 2c) it is possible to identify the occurrence of different lithostratigraphical settings or logs,  
163 expressed by the number of stacked layers each represented in terms of: a) their belonging to the  
164 Bedrock or CT, b) type of *gt\_units* according to conventional classification (e.g., ASTM, 2017), c)  
165 thickness range (Fig. 2d). Therefore, the EGM is a Map where any polygon corresponds to a  
166 preliminary SHM, characterised by the same subsurface lithostratigraphical setting and differs from  
167 a Geological-Geomorphological Map where only the surface geology is represented (Fig. 2e). It is  
168 worth to note that the thickness range includes the lateral variability expected in the microzone and  
169 the experimental uncertainty affecting thickness values assessed (or guessed) in this phase. In  
170 principle, the acquisition of more detailed information (i.e., by geophysical surveys) in the subsequent  
171 step does not necessarily imply a reduction of these ranges since the new data may reduce uncertainty  
172 but confirm or also increase the amount of expected lateral variability within the SHM.



173  
 174 Fig. 2. Description of the EGM assessment methodology. a) Hypothetical CT (a-b-c) and Bedrock (A-B) units as mapped  
 175 on a Geological-Geomorphological Map. Dashed lines represent the traces of the lithostratigraphical cross-sections. b)  
 176 Engineering Geological reclassification of CT and Bedrock units: i.e., SM, Silty sands, mixed sands and silts; GM, Silty  
 177 gravels, mixed gravels, sands and silts; COS, cohesive overconsolidated; LP, lapideous; ls, landslides. Dashed lines  
 178 represent the traces of the lithostratigraphical cross-sections. c) Lithostratigraphical cross-sections according to gt\_unit  
 179 classification. d) Lithostratigraphical logs for each lithostratigraphical setting according to the section and thickness



180 variability for each layer. e) Engineering-Geological Model (EGM), the numbering of the mapped zones (which represent  
181 the preliminary SHMs) corresponds to the numbering of the lithostratigraphical logs.

## 182 **2.2 From EGM to Engineering-Geological/Geophysical Model (EGGM)**

183 In this phase, the aims are twofold. First, new field data corresponding to surface geophysical  
184 prospecting are carried out in order to provide further constraints to the geometries of lithological  
185 bodies delineated in the EGM. Second, these measurements will provide the seismic characterization  
186 of lithostratigraphic units present in the subsoil. Two main elements will be of main interest: a) the  
187 range of ground motion frequencies potentially affected by amplification effects (the ‘resonance  
188 frequencies’,  $f_0$ ), b) Vs values representative of each lithostratigraphic unit identified in the EGM.  
189 The identification of main seismic impedance contrasts and of the identification of the Seismic  
190 Bedrock (SB) will also be of main concern. All these elements play a major role in assessing the local  
191 seismic hazard. SB represents the bottom of the seismo-stratigraphic log responsible for expected  
192 ground motion amplification.

193 The SB may or may not correspond to the Bedrock, depending on its characteristic Vs values. In fact,  
194 for engineering purposes, SB is conventionally defined with Vs values above any threshold ( $> 800$   
195 m/s in Italy by following the Italian Seismic Code NTC, 2018). This definition implies that,  
196 depending upon the geological characteristics and history, not all bedrocks are seismic bedrocks and  
197 eventually also CTs can be SB (i.e., hardly cemented or packed horizons within soft alluvial  
198 sediments). This phase allows the reassessment of representative lithostratigraphical logs for each  
199 polygon of the EGM Map, where the vertical sequence of gt\_units is delineated with more refined  
200 thickness estimate (integrating geological and geophysical observations) along with respective Vs  
201 values (Fig. 1c).

202 Among many other seismic methods, recent practice in Italy (Albarelo et al., 2015; Caielli et al.,  
203 2020) suggests that the ones based on surface waves prospecting procedures (e.g., Foti et al., 2011;  
204 Foti et al., 2017) played a major role in SM studies due to their cost-effectiveness, penetration depth,  
205 applicability in urban contexts. Both active and passive procedures based on single station (Bard,  
206 1999) and array configurations (Okada, 2003; Park, 2011) have been largely used on purpose. A basic  
207 limitation of this approach relies on the strictly 1D interpretation of observations coupled with the  
208 strong non-linearity of the inversion procedure that only allows to define a range of Vs profiles  
209 compatible with observations. This ambiguity cannot be solved by considering the only geophysical  
210 methods but a strong integration of outcomes with geological interpretations is needed for a single  
211 comprehensive model of the subsoil. Anyway, relatively significant uncertainty margins will remain,  
212 which must be accounted for in subsequent analyses.

## 213 **2.3 From EGGM to SHMs Map**

214 The collected data allow to identify homogeneous areas roughly characterized by the same litho- and  
215 seismo-stratigraphical logs. These are: a) outcropping SB with expected AF = 1; b) areas where  
216 ground motion amplification is expected; c) unstable areas (landslides, capable faults, liquefaction).  
217 This methodological step leads to a SM where only stable areas with 1D expected ground motion  
218 amplification are considered for the estimation of AF (eq. 1) that is calculated by suitable tools  
219 (abacuses) in the assumption that (e.g., Paolucci et al., 2020). The possible presence of more complex  
220 effects induced by the local complex geomorphological setting (abrupt slope changes, steep slopes,  
221 narrow ridges, peaks etc..) are also separately parameterized by considering specific abacuses (e.g.,  
222 Ashford and Sitar, 1997; Paolucci, 2002) in the assumption that SB outcrops. Thus, two AFs are  
223 obtained respectively for lithostratigraphical and morphological effects and compared. When

224 morphological AF is comparable or larger than the lithostratigraphical one, a warning is associated  
225 to the relevant site by suggesting more advanced studies.

226 The output of this step is an SHM Map where each polygon is nearly homogeneous in terms of AF:  
227 a) if the same SHM shows a small variability of Amplification Factors (in the range of +/- 0.3, to say)  
228 the geometry of the SHM is confirmed and the relevant log is considered as representative of the  
229 whole SHM; b) where the same SHM shows a relatively large variability of AF then the spatial  
230 geometry of the SHM can change accordingly, i.e., by splitting SHM in more polygons; c) when two  
231 contiguous SHMs show similar AF they can be merged except when the geotechnical properties and  
232 parameters are significantly different.

233 To reach this goal the data collected during the workflow is continuously stored in a spatial database  
234 managed in Geographic Information System (GIS). To this purpose, a database structure has been  
235 developed in Italy [by the](#) Institute of Environmental Geology and Geoenvironment of the National  
236 Research Council (CNR-IGAG) on behalf of the Italian Department for Civil Protection of the  
237 Presidency of Council of Ministers, to store information collected during seismic microzonation  
238 studies by following standardized procedures (DB SM, 2019).

239

### 240 **3. CASE STUDY**

#### 241 **3.1 Geographic, Geological and Geomorphological background**

242 The study area is located in the Umbro-Marchean Apennine (Central Italy, Marche Region; Fig. 3a),  
243 an east-north-east verging fold-and-thrust belt developed due to the collision between the African and  
244 European plates (Boccaletti et al. 1990; Cavazza et al. 2004; Cosentino et al. 2010 and bibliography  
245 therein). The geological and geomorphological setting is the result of the complex interaction between  
246 the Meso-Cenozoic stratigraphy and structural evolution and the Quaternary tectonic uplift that led  
247 to the modelling of the present-day landscape (Calamita et al., 1999; Coltorti and Pieruccini, 1999).

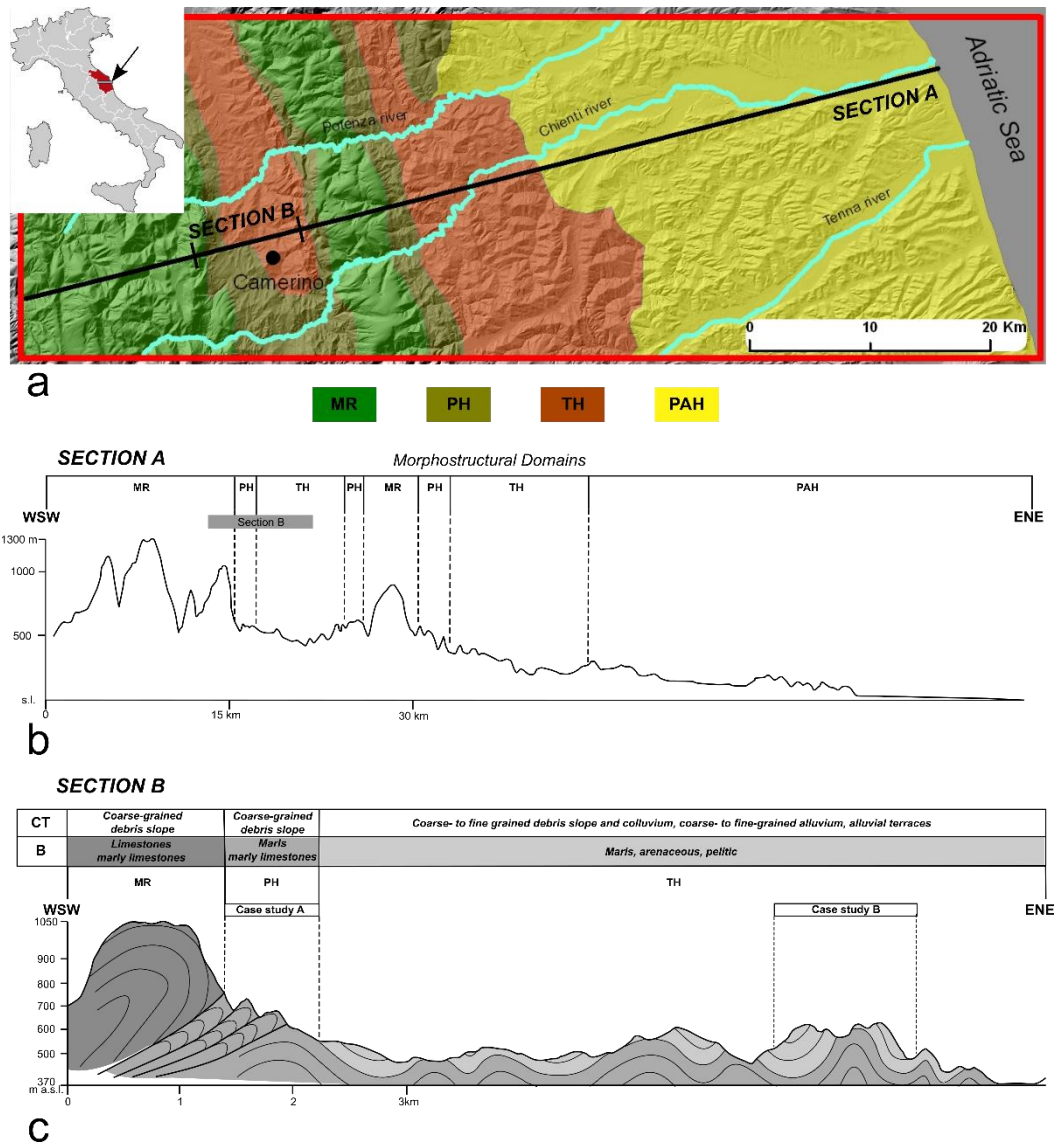
248 Therefore, different morphostructural domains can be recognised at regional scale (Fig. 3a,b). They  
249 are characterised by distinctive geological and structural settings, peculiar morphological features  
250 and by different types of Bedrock and CTs (Amanti et al., 2020) described in the follows.

251 Mountain Ridges are characterised by elevations exceeding 2000 m a.s.l. and with steep to very steep  
252 slopes modelled on Bedrocks made of mainly calcareous Triassic-Oligocene formations belonging to  
253 the Umbro-Marchean succession (Centamore et al., 1986). Also, Mountain Ridges are bounded to the  
254 north-east by Miocene overthrusts (Fig. 3b) (Calamita and Deiana, 1988) and therefore the Bedrock  
255 is here commonly strongly fractured and weathered. The geomorphological processes associated to  
256 the landscape modelling led to the incision of deep valleys and to the deposition of shallow to thick  
257 CTs made of mostly coarse-grained alluvial and slope sediments.

258 Pedemountains Hills, characterized by gentle to steep slopes and elevations up to 1000 m a.s.l., are  
259 located to the NE and the SW of the MRs; the Bedrock is mainly made of alternating Oligocene-  
260 Miocene marls and limestones (Centamore et al., 1986) disturbed by the presence of overthrusts  
261 systems. CTs are dominated by coarse-grained alluvial and slope deposits and the valleys are wider  
262 than in Mountain Ridges and the slopes are affected by frequent gravity phenomena.

263 Terrigenous Hills, with elevations generally lower than 800 m a.s.l., have gentler slopes than  
264 Mountain Ridges and Pedemountains Hills and the Bedrock is mostly made of Messinian sandstones  
265 and clays belonging to foredeep siliciclastic turbiditic basins (Centamore et al., 1991) usually folded  
266 and faulted with local associated fracturing. CTs are mainly made of finer-grained slope and colluvial  
267 sediments and by coarse- to fine-grained alluvial deposits forming fluvial terraces within wide valley  
268 systems.

269 Periadriatic Hills, with elevations progressively decreasing toward the Adriatic coastline, are  
 270 characterised by gentle slopes modelled on a Bedrock made of Pliocene-Lower Pleistocene marine  
 271 clays and sands of the Periadriatic Basin (Bigi et al. 1997), deformed by gentler folds and only minor  
 272 faults. CTs are fine-grained slope and colluvial deposits and coarse- to fine-grained alluvial sediments  
 273 forming fluvial terraces within valleys that become progressively wider toward the coast.  
 274 The overall setting indicates the progressive change of engineering geological characteristics of  
 275 Bedrocks from mainly lapideous (Mountain Ridges), to alternated lithologies (Pedemountain Hills),  
 276 to granular (Terrigenous Hills) to overconsolidated cohesive and granular (Periadriatic Hills). Also,  
 277 CTs characteristics change according to the distribution of the Bedrocks.  
 278 The case study are settlements located within Pedemountain Hills and Terrigenous Hills (respectively  
 279 case study A and B in Fig. 3c) domains in the so-called Camerino Basin characterised by a strong  
 280 historical seismic activity culminated with the 2016-2017 seismic sequence and associated damages  
 281 (Galli et al., 2017). These localities are representatives of the geological-geomorphological contexts  
 282 and settlement systems typical of the Northern Apennine where small historical villages are scattered  
 283 in the landscape according to favourable topographic, land-use and climatic conditions.



284 Fig. 3. a) The Morphostructural domains of the Umbro-Marchean Apennine (from Amanti et al., 2020 modified). MR –  
 285 Mountain Ridges; PH – Pedemountain Hills; TH – Terrigenous Hills; PAH – Periadriatic Hills. b) Topographic section  
 286 (section A) across the area with the indication of the Morphostructural domains. c) Simplified geological section across  
 287

288 the study area (section B) with the indication of the Morphostructural domains and the main types of Cover Terrains (CT)  
 289 and Bedrock (B). The location of case studies is also reported.

### 290 3.2 The Engineering-Geological Model (EGM)

291 The EGM is assessed for the surrounding of the settlements following a Geological-  
 292 Geomorphological analysis of a wider context for each morphostructural domain under study. The  
 293 geological units (formal and informal lithostratigraphical units) are then reclassified and coded  
 294 following their main engineering geological properties in terms of gt\_units (Table 1).

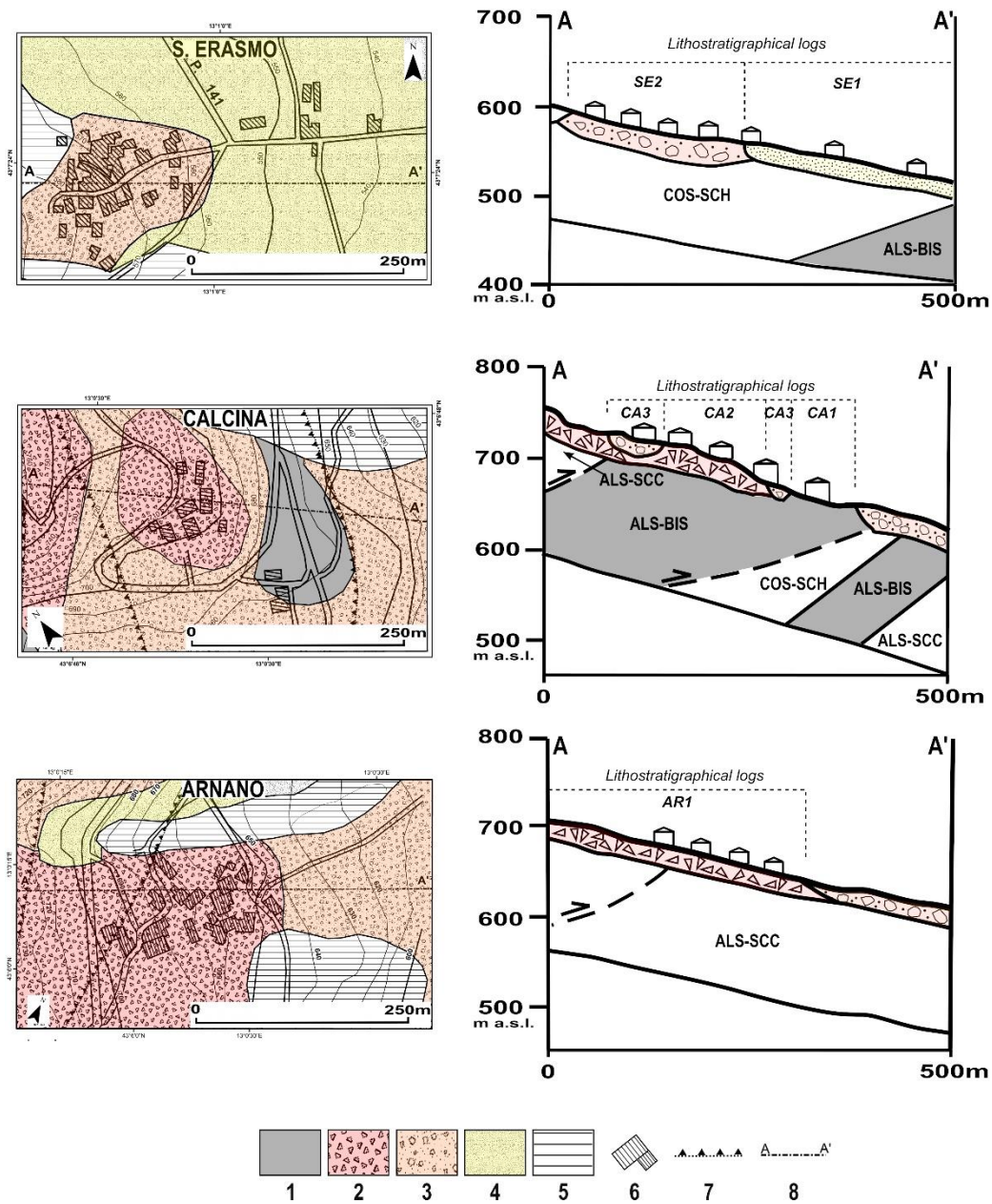
	Geological Unit	Description	gt_code	gt_unit description
CT	Eluvial-colluvial deposits (Holocene)	Unsorted, loose to packed, mostly fine-grained deposits	ML	Inorganic silts, fine silty-clayey sands, low plasticity clayey silts
	Debris-slope deposits (Holocene)	Unsorted, loose to packed, angular to subangular, calcareous debris	GP	Not sorted gravels, mixed gravels and sands
	Debris-slope deposits (Late Pleistocene)	Unsorted, weakly to strongly cemented, angular to subangular calcareous debris	GP	Not sorted gravels, mixed gravels and sands
	Alluvial deposits (Late Pleistocene)	Unsorted, packed, subangular to rounded alluvial gravels and sands	GM	Silty gravels, mixed gravels, sands and silts
B	Camerino Formation FCi	Pelitic-arenaceous lithofacies	COS	cohesive overconsolidated
	Camerino Formation FCId	Arenaceous lithofacies	GRS	grainy cemented stratified
	Schlier Formation SCH	Marls and clays	COS	cohesive overconsolidated
	Biscliaro Formation BIS	Marly limestones, marls and limestones	ALS	alternations of contrasting lithotypes
	Scaglia Cinerea Formation SCC	Limestones and marls	ALS	alternations of contrasting lithotypes

295

296 Table 1. Engineering geological reclassification of the Geological units in the study area: CT, Cover Terrains; B,  
 297 Bedrock.

#### 298 3.2.1 EGM Pedemountain Hills: S.Erasmo-Calcina-Arnano (case study A)

299 The area is characterised by the presence of 3 small settlements aligned at the north-eastern foot  
 300 slopes of a Mountain Ridge reaching 1500 m asl in elevation (Fig. 3c). EGM is described for the  
 301 immediate surroundings of the settlements and based on the Geological-Geomorphological map made  
 302 by integrating existing data and ad hoc field surveys, lithostratigraphical cross sections (Fig. 4) and  
 303 lithostratigraphical logs (Fig. 5) representative of the preliminary SHMs. In this step, gt\_unit  
 304 thickness ranges are preliminary assessed. The main structural feature is the presence of a series of  
 305 thrusts affecting the Bedrock made of the uppermost marly-calcareous and marly-clayey formations  
 306 of the Umbro-Marchean succession (Fig. 3c). The slopes are from medium to very steep, and  
 307 characterised by two main generations of coarse-grained CTs, packed and locally cemented (Late  
 308 Pleistocene) or poorly packed to loose (Holocene). Only in Calcina (Fig. 4 and Fig. 5) the two  
 309 generations of debris slope deposits are superimposed. In S.Erasmo (Fig. 4 and Fig. 5) CTs are also  
 310 made of a thin layer of poorly sorted, loose sandy-silty colluvial sediments related to the weathering  
 311 of the marly-clayey Bedrock. The basal contact between CTs and the Bedrock is undulated or planar.  
 312 The slopes are also affected by large- to medium-sized complex gravity phenomena.



313

314 Fig. 4. Case study A, Engineering Geological Maps (left) and lithostratigraphical cross-sections (right) with  
 315 correspondence to the lithostratigraphical logs of Fig. 5. For the engineering technical classification of gt\_units see  
 316 Table 1). Legend: 1 – Bedrock ALS; 2 – CT GP; 3 – CT GP; 4 – CT ML; 5 - Landslides; 6 - Buildings; 7 – Buried  
 317 overthrusts; 8 – Trace of geological section.

SE - S.ERASMO						AR - ARNANO											
log id	Min (m)	Max (m)	B/CT	gt code	Description	log id	Min (m)	Max (m)	B/CT	gt code	Description	log id	Min (m)	Max (m)	B/CT	gt code	Description
1	2	5	CT	ML	Unsorted low plasticity silts, clays and sands	2	5	25	CT	GP	Angular to subangular unsorted calcareous debris-slope, weakly to strongly cemented	1	5	20	CT	GP	Angular to subangular unsorted calcareous debris-slope, weakly to strongly cemented
	30	140	B	COS	Marls and clays (SCH Fm)												
	10	70	B	ALS	Marly limestones (BIS Fm)												
CA - CALCINA																	
log id	Min (m)	Max (m)	B/CT	gt code	Description	log id	Min (m)	Max (m)	B/CT	gt code	Description	log id	Min (m)	Max (m)	B/CT	gt code	Description
1	70	100	B	ALS	Marly limestones (BIS Fm)	2	5	25	CT	GP	Angular to subangular unsorted calcareous debris-slope, weakly to strongly cemented	3	5	15	CT	GP	Angular to subangular, loose, unsorted calcareous debris
				COS	Marls and clays (SCH Fm)								B	ALS	Marly limestones (BIS Fm)	5	25
	10	20		ALS	Marly limestones (BIS Fm)		B	ALS	Marly limestones (BIS Fm)								
5	30	ALS	Marly limestones (BIS Fm)														

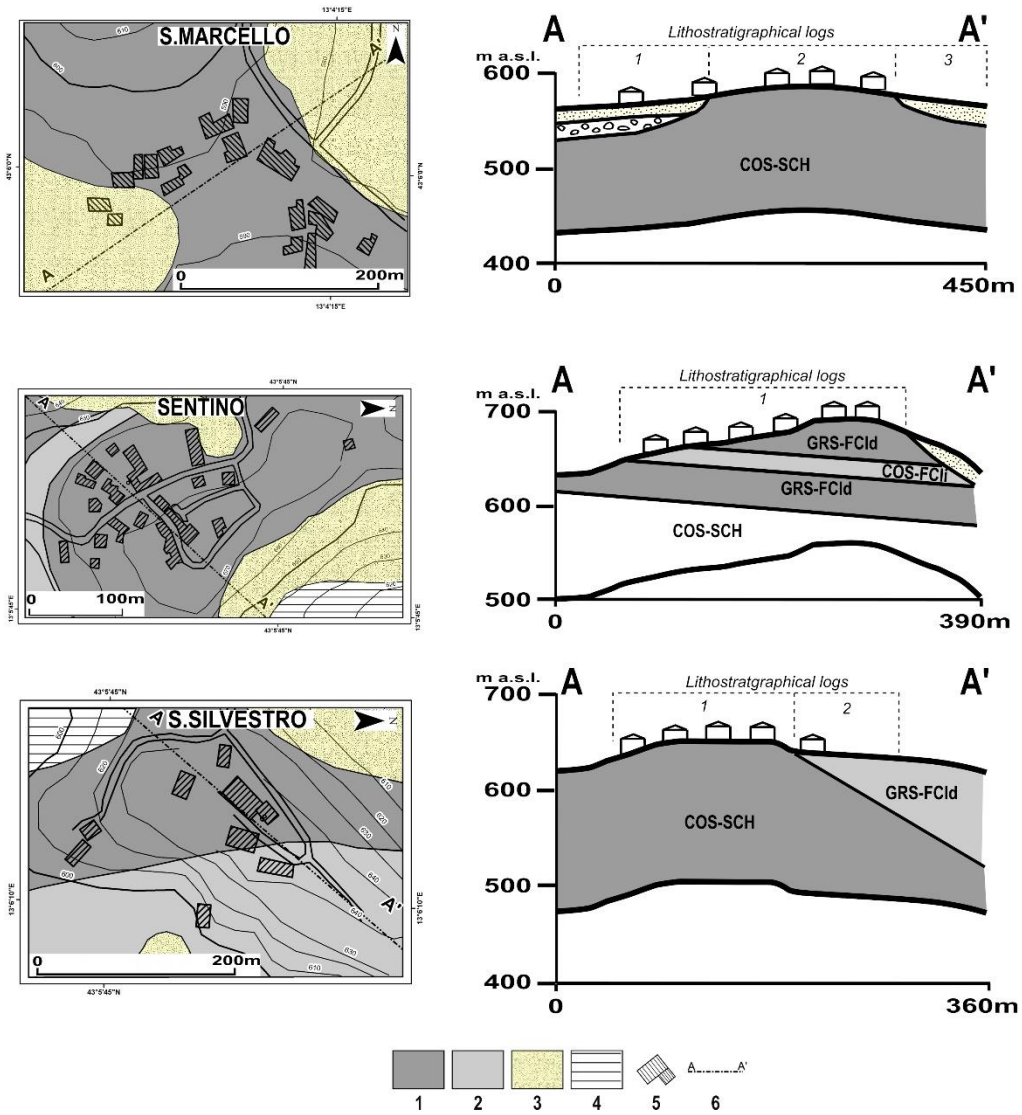
318  
319

320 *Fig. 5. Lithostratigraphical logs in S.Erasmo, Arnano and Calcina (Fig. 4). B: Bedrock; CT: Cover Terrains; gt\_units:*  
321 *engineering technical classification (see Table 1); SCH, Schlier Fm; BIS Bisciario Fm; SCC, Scaglia Cinerea Fm. The*  
322 *columns "Min" and "Max" identify the thickness ranges preliminarily associated to the geological units.*

323 **3.2.2 EGM Terrigenous Hills: S.Marcello-Sentino (case study B)**

324 The area (Fig. 3c) is characterised by the presence of small settlements distributed on 3 different  
325 geomorphological setting: S.Marcello is located on a wide saddle at the head of a valley, Sentino and  
326 S.Silvestro over a hilltop (Fig. 6). The folded Bedrock is made of the Late Miocene marly-clayey and  
327 terrigenous rocks belonging to the Umbro-Marchean succession and Camerino Basin (SCH and FCI  
328 Fms). The slopes are gently steep to very steep, locally with stepped profiles due to selective erosion  
329 on the more resistant arenaceous Bedrock and the marly-clayey slopes are affected by shallow  
330 landslides. In S.Marcello, the wide saddle forms a wind gap belonging to a palaeo-drainage as  
331 confirmed by the presence of an alluvial gravelly horizon buried under recent colluvial deposits on  
332 the south-western slope (Fig. 6). In Sentino and S.Silvestro, CTs are very shallow (less than 2 m) or  
333 lacking on the steep slopes surrounding the settlements, mostly due to erosional runoff processes and  
334 anthropic activities (Fig. 6).

335



336

337 Fig. 6. Case study B, Engineering Geological Maps and lithostratigraphical cross-sections with correspondence to the  
 338 lithostratigraphical logs of Fig. 7. Legend: 1 – Bedrock COS; 2 – Bedrock GRS; 3 – CT: ML; 4 - Landslides; 5 - Buildings;  
 339 6 – Trace of geological section.

SM - S.MARCELLO																						
log id	Min (m)	Max (m)	B/CT	gt code	Description	log id	Min (m)	Max (m)	B/CT	gt code	Description	log id	Min (m)	Max (m)	B/CT	gt code	Description					
1	3	10	CT	ML	Holocene fine-grained unsorted eluvial and colluvial deposits	2					Marls and clays (SCH Fm)	3	3	10	CT	ML	Holocene fine-grained unsorted eluvial and colluvial deposits					
	3	15	CT	GM	Pleistocene alluvial packed unsorted gravels and sands																	
				B	COS		Marls and clays (SCH Fm)			B			COS	Marls and clays (SCH Fm)								
SN - SENTINO						SS - S.SILVESTRO																
log id	Min (m)	Max (m)	B/CT	gt code	Description	log id	Min (m)	Max (m)	B/CT	gt code	Description	log id	Min (m)	Max (m)	B/CT	gt code	Description					
1	3	50	B	GRS	Arenaceous lithofacies (FCId Fm)	1					Marls and clays (SCH Fm)	2					Arenaceous lithofacies (FCId Fm)					
	15	15	B	COS	Pelitic-arenaceous lithofacies (FCII Fm)										3	100		B	GRS	Arenaceous lithofacies (FCId Fm)		
	3	30	B	GRS	Arenaceous lithofacies (FCId Fm)																	
				B	COS		Marls and clays (SCH Fm)													B	COS	Marls and clays (SCH Fm)

340  
341  
342  
343  
344

Fig. 7. Lithostratigraphical logs in S.Marcello, Sentino and S.Silvestro (Fig. 6). B: Bedrock; CT: Cover Terrains; gt\_units: engineering technical classification (see Table 1); SCH, Schlier Fm; FCId, Camerino Fm; FCII, Camerino Fm. The columns "Min" and "Max" identify the thickness ranges preliminarily associated to the geological units.

345

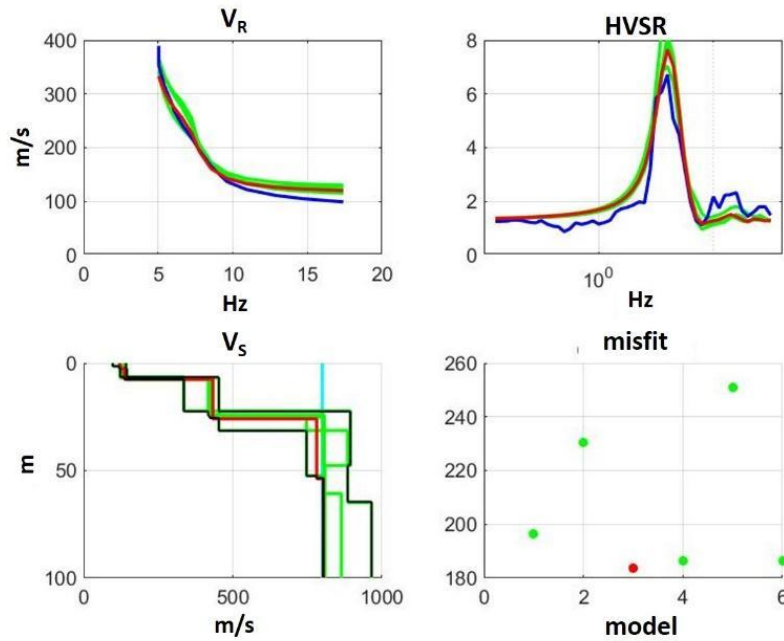
### 3.3 From EGM to EGGM

346  
347  
348  
349  
350  
351  
352  
353  
354  
355  
356  
357  
358  
359  
360  
361  
362

Geophysical surveys have been carried out in the study area to support geological analysis and provide the seismic parameterization of the gt\_units present in the study area. To this purpose, both active and passive seismic prospecting were performed. The siting of these measurements was optimized by considering the preliminary EGM described above. Both active and passive prospecting techniques have been considered. Several single station measurements of ambient vibrations (see, e.g., Bonnefoy-Claudet et al., 2006) were performed to identify soil resonance frequency  $f_0$  by the HVSR technique (e.g., Lachet and Bard, 1994; Bard, 1999). Array measurements (both in active and passive configurations) have been also carried out to infer representative Vs profiles from Rayleigh waves dispersion curves. MASW and ESAC/FK/MSPAC procedures were respectively used when active and passive configurations were respectively considered to determine the Rayleigh wave dispersion curve (e.g., Okada, 2003; Park, 2011; Foti et al., 2017). The choice between the two approaches depended on the specific situation: when deeper soft sedimentary covers were expected, the passive array has been preferred to the active one because of its greater penetration depth. As a whole, 103 HVSR measurements and 22 array surveys (22 active and at 7 sites accompanied by passive acquisitions) have been carried out in the study area. To retrieve the Vs profiles, assess the depth of main seismic impedance contrasts and SB as well as attributing representative seismic parameters to the gt\_units, outcomes of the HVSR and array measurements were jointly inverted by



363 using Genetic Algorithm, Monte Carlo or Simulated Annealing inversion procedure (e.g., Arai and  
 364 Tokimatsu, 2005; Albarello et al., 2011; Garcia-Jerez et al., 2016). In order to explore possible  
 365 uncertainty in the final outcome, the inversion has been carried out a number of times by retrieving  
 366 each time the best fitting solution (e.g., Albarello et al., 2017). In Fig. 8, an example of results  
 367 provided by the inversion process is reported as concerns colluvial deposits in the S. Marcello site  
 368 (Fig. 7). One can see that a sharp seismic impedance contrast is detected around 25 m of depth at the  
 369 bottom of the colluvial cover and that the range of experimental uncertainty is quite small.



370  
 371 *Fig. 8. Outcomes of the inversion of single station and array measurements at the S. Marcello site. In the figures at the*  
 372 *top line, the experimental Rayleigh wave velocity ( $V_R$ ) dispersion (top left) and HVSR (top right) curves are reported in*  
 373 *blue. In these figures, theoretical curves provided by considering the models obtained by the inversion runs are reported*  
 374 *in green. In red the overall best fitting solution is plotted. The corresponding misfit values are reported in the right figure*  
 375 *at the bottom line. The  $V_s$  profiles corresponding to these runs are reported in right figure at the bottom. Black continuous*  
 376 *lines indicate the confidence interval for the  $V_s$  values. The vertical light-blue line indicates the value corresponding to*  
 377 *the conventional SB (800 m/s).*

378 By considering outcomes of the geophysical survey, the gt\_units present in the study area have been  
 379 parameterized in terms representative thickness and  $V_s$  values (Fig. 9 and Fig. 10). In particular, in  
 380 order to account for the expected lateral variations and experimental uncertainty, a range of possible  
 381 values is attributed to both these parameters.

### 382 3.3.1 PH Pedemountain Hills

383 In most cases (Fig. 9) there is a good correspondence between the EGM and the observed geophysical  
 384 parameters in terms of layer thicknesses. The total thickness range of the CT's recognised in the EGM  
 385 was over- or under-estimated but comparable with their expected lateral variability, ranging about  
 386 10-50% according to the availability or to the lack of suitable and reliable existing data. In Calcina 2  
 387 (Fig. 9), the CT layer was re-defined by 3 seismic layers according to the  $V_s$  value although within  
 388 the same lithostratigraphical unit. Finally, an important contrast of impedance marks the boundary  
 389 between CTs and the SB. In Calcina 2 and 3 (Fig. 9) the Bedrock (ALS-BIS Fm), buried under CTs,  
 390 shows  $V_s$  values  $>800$  m/s and therefore considered as SB. In Calcina 1 (Fig. 9) the outcropping  
 391 Bedrock (ALS-BIS Fm) shows  $V_s$  values  $<800$  m/s and a progressive increase of velocity with depth,  
 392 reaching values greater than 800 m/s at about 40 m and the impedance contrast is within the Bedrock.





438 three AFs are defined for each microzone relative to three ranges of building resonance periods (0.1-  
 439 0.5s, 0.4-0.8s, 0.7-1.1s) by considering three pieces of information:

- 440 1. the geological domain (*sensu* Paolucci et al., 2020);
- 441 2. the SB depth;
- 442 3. the average  $V_s$  value to the SB (or to 30 m if the SB is deeper);
- 443 4. the fundamental soil resonance frequency  $f_0$  estimated from HVSR measurements.

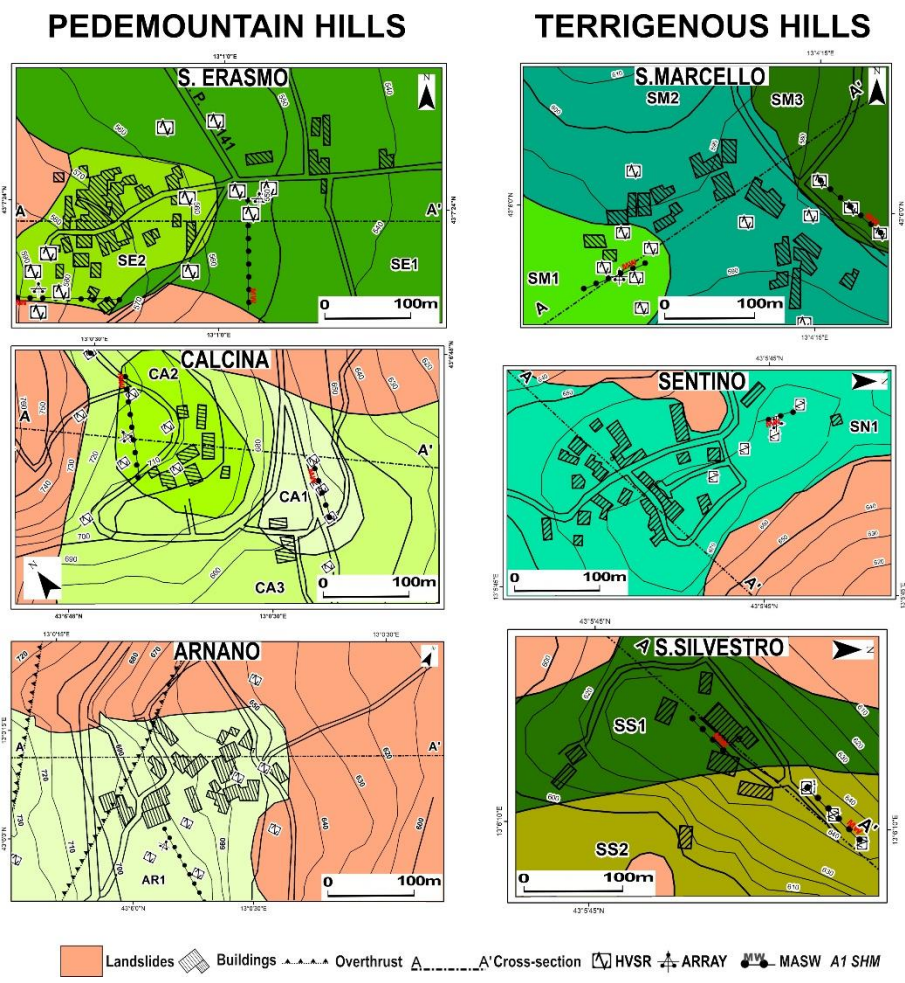
444 As one can see all the above parameters can be deduced from the EGGM. This also implies that  
 445 several FA values could be obtained for the same microzone in the case that several  $f_0$  measurements  
 446 have been performed in that zone. Eventual significant differences among the FA values for the same  
 447 microzone could suggest that lateral variations exist (eventually considered as negligible in the  
 448 previous phases), which may result in significant differences in the local seismic hazard. This may  
 449 suggest the splitting of the relevant microzone to identify new microzones more homogeneous in  
 450 terms of relative hazard. If within the SHM no ground motion amplification is expected, i.e., where  
 451 SB outcrops or where CTs or Bedrock are characterized by thicknesses lower than 3 m, the relevant  
 452 AFs assume values equal to 1. In the case studies, the possible presence of morphological  
 453 amplification effects has been evaluated and shown to be negligible.

454 By considering these elements, the relevant AF values have been computed for both case studies  
 455 (Table 2). The final SHM Maps are reported in Fig. 11. Observing the AF values and Fig. 9 and Fig.  
 456 10, it is possible to note that the highest ones (considering all the period ranges) are associated to the  
 457 SHMs where the layers above the SB are characterized by the lowest  $V_s$  values. No significant  
 458 differences appear to be related to the SB depth. S.Marcello 2 (SM 2) and S.Silvestro 1 (SS 1) are  
 459 two SHMs where no ground motion amplification is expected. Moreover, no significant differences  
 460 emerged between the estimate of AF values within the same SHM and thus it was not necessary to  
 461 change geometry of the SHMs. Implicitly, thus outcome supports effectiveness of the EGGM model  
 462 in the context of this case study.

SHM	AF 0.1-0.5 s	AF 0.4-0.8 s	AF 0.7-1.1 s
SE 1	2.2	2.5	2.3
SE 2	2.4	2.5	2.3
CA 1	1.5	1.5	1.3
CA 2	1.6	1.8	1.8
CA 3	2.6	1.8	1.5
AR 1	1.4	1.3	1.1
SM 1	2.5	2	1.4
SM 2	1	1	1
SM 3	2.4	2	1.4
SN 1	1.6	1.8	1.5
SS 1	1	1	1
SS 2	1.6	1.5	1.4

463

464 *Table 2. AF values estimated using the abacuses for the SHMs belonging to the Pedemountain Hills considering the three*  
 465 *period ranges. SE – S.Erasmo; CA – Calcina; AR – Arnano; SM – S.Marcello; SN – Sentino; SS – S.Silvestro.*



466

467 *Fig. 11. SHM Maps of the case studies. The grey colours are referred to the SHMs described in Fig. 9, Fig. 10 and Table*  
 468 *2.*

469 **5. CONCLUSIONS**

470 Several seismic microzonation procedures have been applied worldwide in the last years (e.g.,  
 471 Thitimakorn, 2019; Molnar et al., 2020; Régnier et al. 2020; Salsabili et al., 2021; Mase et al., 2021)  
 472 by considering both geological and geophysical/geotechnical information to constrain expected  
 473 amplification effects. In most cases, engineering geological information plays a minor qualitative role  
 474 and no specific protocol is defined to standardize its implementation in microzonation studies. This  
 475 last issue is the aim of the present contribution. In particular, a workflow has been delineated aiming  
 476 at providing a methodological basis for a full integration of geological/geomorphological and  
 477 geophysical protocols for the seismic characterization of wide areas (Seismic Microzonation). The  
 478 first main goal of this methodological approach is obtaining maximum results by minimizing costs.  
 479 This makes the proposed approach feasible also where economic resources are scarce (small  
 480 settlements, developing countries, etc.). In this view, the assessment of a reliable Engineering-  
 481 Geological Model (in the perspective of seismic response analysis) is of main importance to assess a  
 482 three-dimensional distribution of lithostratigraphical settings, to orient geophysical surveys and to  
 483 provide a coherent interpretative framework. The workflow here proposed includes three steps: a) the  
 484 development of a 3D reference engineering geological model resulting in the partition of the study  
 485 area into homogeneous microzones (in the perspective of hazard assessment), b) the refinement of  
 486 this model by considering outcomes of on-purpose geophysical surveys and the seismic  
 487 parameterization of the microzones, c) the preliminary quantification of expected amplification the  
 488 phenomena in each microzone. The results show as the evaluated AF are consistent with the EGGM

489 emphasizing the importance of a well-established model that *de facto* makes simpler the evaluation  
490 of seismic hazard. The results of this approach are of paramount importance for land planning and  
491 particularly in the framework of restoration policies. In fact, despite the approximate character of  
492 hazard estimates, outcomes will also allow the identification of areas where the expected  
493 enhancement of seismic ground motion may suggest detailed seismic response studies before  
494 planning new constructions. This approach to local seismic hazard assessment cannot be considered  
495 as alternative to site specific seismic response studies required by seismic regulations for anti seismic  
496 design of single buildings. Anyway, it may provide useful constraints for these studies. In particular,  
497 information provided by Seismic Microzonation may be useful to assess the dimension of the volume  
498 of subsoil (the “site domain” defined by IAEA, 2016) to be characterized in detail to provide effective  
499 numerical estimates of the local seismic response.

500

## 501 **ACKNOWLEDGEMENTS**

502 We are grateful to Silvia Marchese, Valerio Ferrazza and Michele Amaddii for their help in  
503 performing geophysical and geological/geomorphological surveys in the investigated areas.  
504 Vincenzo Amato and the other anonymous referee also provided encouraging comments and  
505 suggestions to improve the paper. The work has been developed in the frame of scientific activity of  
506 the Center for Seismic Microzonation and Applications  
507 (<https://www.centromicrozonazioneismica.it/en/>)

508

## 509 **DECLARATIONS**

510 Funding: Not applicable  
511 Conflicts of interest/Competing interests: Not applicable  
512 Availability of data and material: Not applicable  
513 Code availability: Not applicable  
514 Authors' contributions (optional: please review the submission guidelines from the journal whether  
515 statements are mandatory)

516

## 517 **REFERENCES**

- 518 Albarello, D., Cesi, C., Eulilli, V., Guerrini, F., Lunedei, E., Paolucci, E., Pileggi, D., Puzzilli, L.M.,  
519 2011. The contribution of the ambient vibration prospecting in seismic microzoning: an example  
520 from the area damaged by the 26th April 2009 L’Aquila (Italy) earthquake. *Boll.Geofis.Teor.Appl.*  
521 52, 513-538. <https://doi.org/10.4430/bgta0013>.
- 522 Albarello, D., Socco, L.V., Picozzi, M., Foti, S., 2015. Seismic Hazard and land management policies  
523 in Italy: the role of seismic investigations. *First Break* 33, 87-93. <https://doi.org/10.3997/1365-2397.33.8.82009>.
- 525 Albarello, D., Francescone, M., Lunedei, E., Paolucci, E., Papasidero, M.P., Peruzzi, G., Pieruccini,  
526 P., 2017. Seismic characterization and reconstruction of reference ground motion at accelerometric  
527 sites of the Italian national accelerometric network (RAN). *Nat Hazards* 86, 401-416.  
528 <https://doi.org/10.1007/s11069-016-2310-4>.

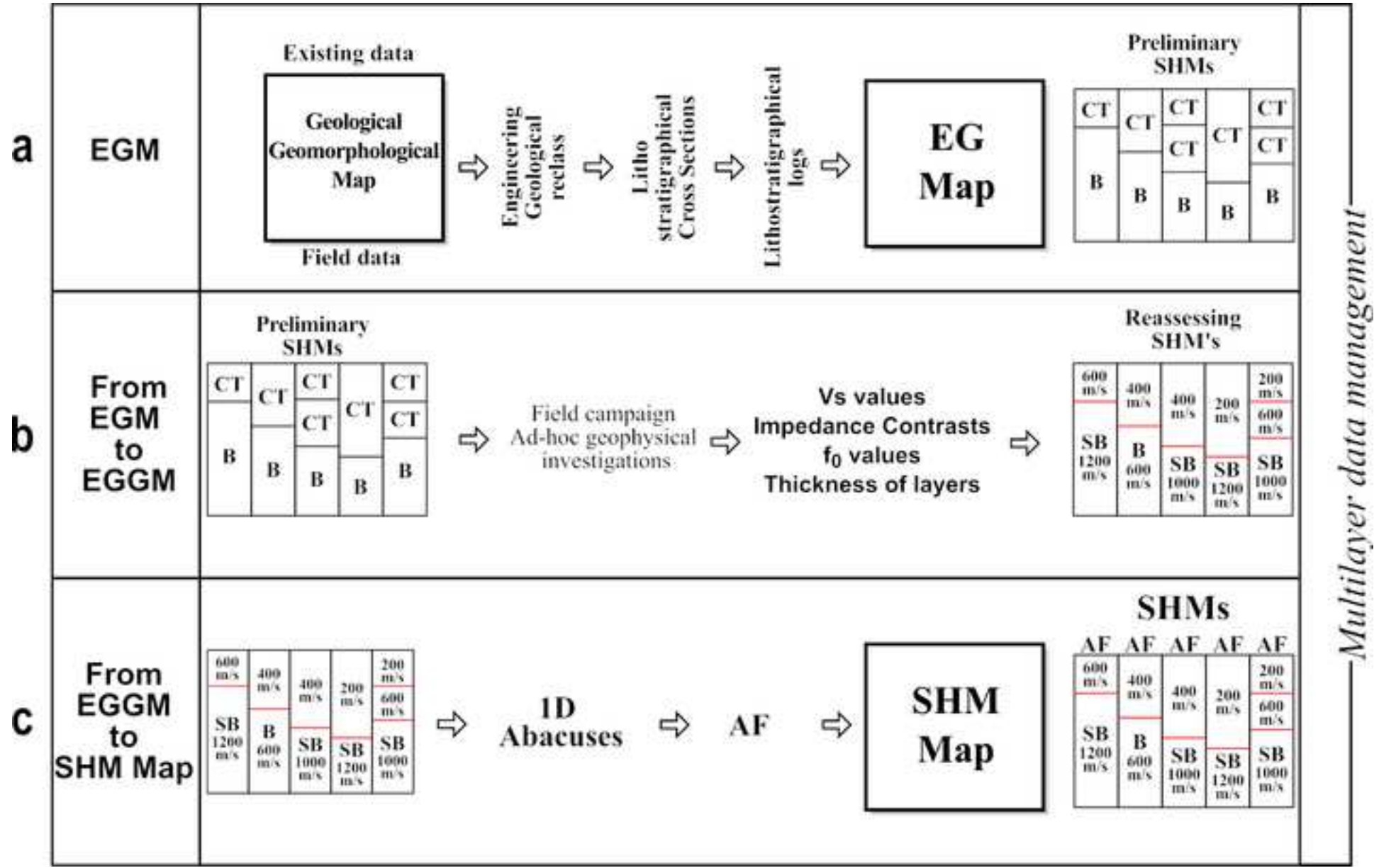
- 529 Albarello, D., 2017. Extensive application of seismic microzoning: methodological and socio-  
530 political issues in the Italian Experience. *Boll.Geofis.Teor.Appl.* 58, 4, 253-264. DOI  
531 10.4430/bgta0205.
- 532 Amanti, M., Chiessi, V., Muraro, C., Puzzilli, L.M., Roma, M., Catalano, S., Romagnoli, G.,  
533 Tortorici, G., Cavuoto, G., Albarello, D., Fantozzi, P.L., Paolucci, E., Pieruccini, P., Caprari, P.,  
534 Mirabella, F., Della Seta, M., Esposito, C., Di Curzio, D., Francescone, M., Pizzi, A., Macerola,  
535 L., Nocentini, M., Tallini, M., 2020. Geological and geotechnical models definition for 3rd level  
536 seismic microzonation studies in Central Italy. *Bull.Earthq.Eng.* 18, 5441-5473.  
537 <https://doi.org/10.1007/s10518-020-00843-x>.
- 538 Arai, H., Tokimatsu, K., 2005. S-wave velocity profiling by joint inversion of microtremor dispersion  
539 curve and horizontal-to-vertical (H/V) spectrum. *Bull. Seismol. Soc. Am.* 95, 5, 1766-1778.  
540 <https://doi.org/10.1785/0120040243>.
- 541 Ashford, S.A., Sitar, N., 1997. Analysis of topographic amplification of inclined shear waves in a  
542 steep coastal bluff. *Bull.Seismol.Soc.Am.* 87, 692-700.
- 543 ASTM, 2017. Standard Practice for Classification of Soils for Engineering Purposes (Unified Soil  
544 Classification System), ASTM International, West Conshohocken, PA, [www.astm.org](http://www.astm.org).
- 545 Baratta, M., 1910. La catastrofe sismica calabro messinese : 28 dicembre 1908. Società geografica  
546 italiana, reprinted by Forni, 1985, Bologna (in Italian).
- 547 Bard, P.Y., 1999. Microtremor measurements: a tool for site effect estimation? In: Irikura, K., Kudo,  
548 K., Okada, H., Sasatani, T. (Eds.), *The effects of surface geology on seismic motion*. Balkema,  
549 Rotterdam, pp. 1251–1279. ISBN 90 5809 0302.
- 550 Bigi, S., Cantalamessa, G., Centamore, E., Didaskalou, P., Micarelli, A., Nisio, S., Pennesi, T.,  
551 Potetti, M., 1997. The periadriatic basin (Marche-Abruzzi sector, Central Italy) during the Plio-  
552 Pleistocene. *Giorn. Geol.* 59, 245-259.
- 553 Boccaletti, M., Calamita, F., Deiana, G., Gelati, R., Massari, F., Moratti, G., Ricci Lucchi, F., 1990.  
554 Migrating foredeep-thrust belt system in the Northern Apennines and Southern Alps. *Paleo. Paleo.*  
555 *Paleo* 77, 3-14. [https://doi.org/10.1016/0031-0182\(90\)90095-O](https://doi.org/10.1016/0031-0182(90)90095-O).
- 556 Bonnefoy-Claudet, S., Cotton, F., Bard, P.Y., 2006. The nature of noise wavefield and its applications  
557 for site effects studies: a literature review. *Earth. Sci. Rev.* 9, 205-227.  
558 <https://doi.org/10.1016/j.earscirev.2006.07.004>.
- 559 BSSC NEHRP, 2000. Recommended Provisions for Seismic Regulations for New Buildings and  
560 Other Structures. 2000 Edition, Building Seismic Safety Council for the Federal Emergency  
561 Management Agency (FEMA Rep. 368, 369), Part 1: Provisions (FEMA Report 368); Part 2:  
562 Commentary (FEMA Report 369), Washington, D.C.
- 563 Caielli, G., De Franco, R., Di Fiore, V., Albarello, D., Catalano, S., Pergalani, F., Cavuoto, G.,  
564 Cercato, M., Compagnoni, M., Facciorusso, J., Famiani, D., Ferri, F., Imposa, S., Martini, G.,  
565 Paciello, A., Paolucci, E., Passeri, F., Piscitelli, S., Puzzilli, L.M., Vassallo, M., 2020. Extensive  
566 surface geophysical prospecting for seismic microzonation. *Bull.Earthq.Eng.* 18, 5475-5502.  
567 <https://doi.org/10.1007/s10518-020-00866-4>.
- 568 Calamita, F., Deiana, G., 1988. The arcuate shape of the Umbria-Marche-Sabina Apennines (Central  
569 Italy). *Tectonophysics* 146, 139–147. [https://doi.org/10.1016/0040-1951\(88\)90087-X](https://doi.org/10.1016/0040-1951(88)90087-X).

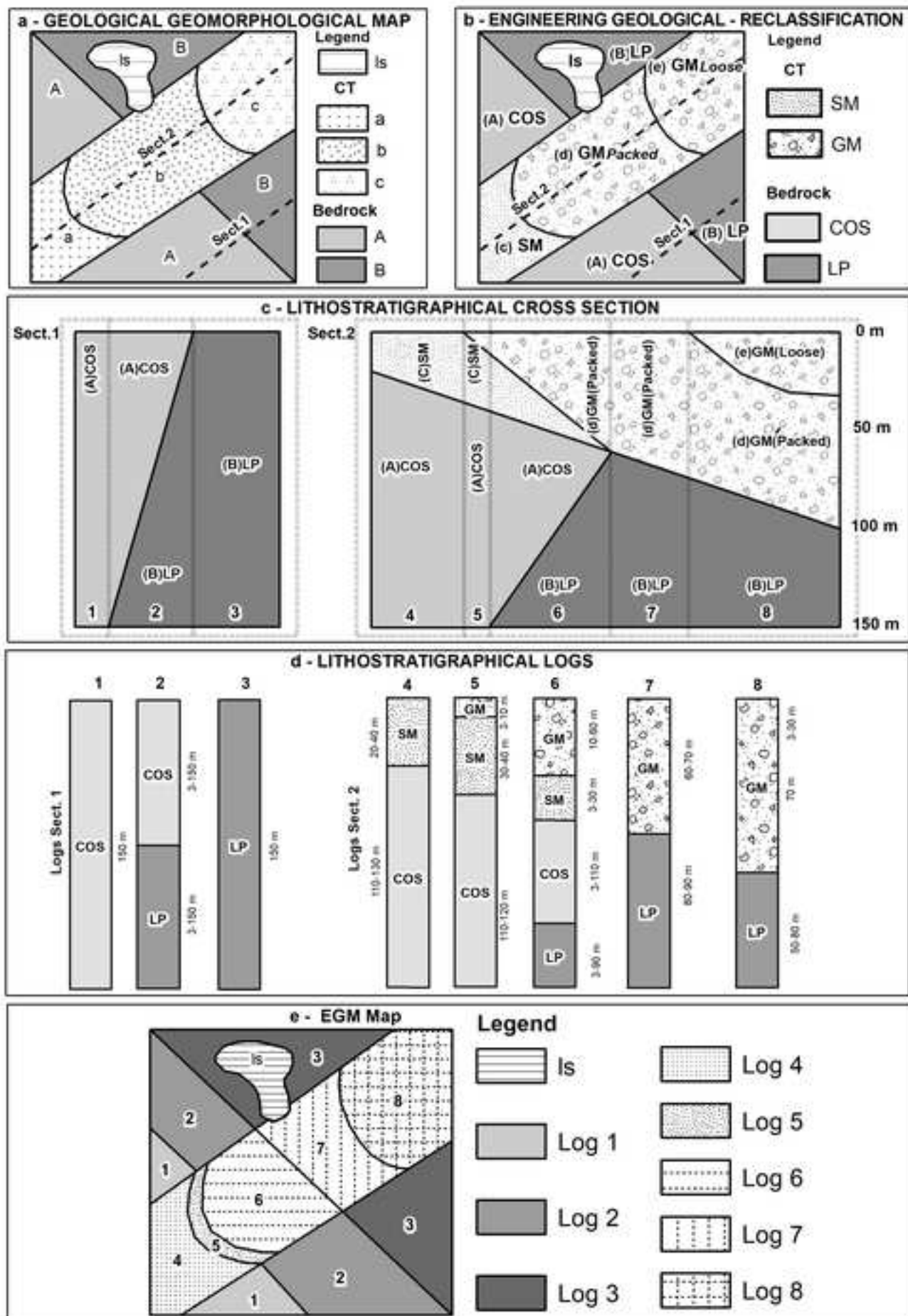
- 570 Calamita, F., Coltorti, M., Pieruccini, P., Pizzi, A., 1999. Evoluzione strutturale e morfogenesi plio-  
571 quaternaria dell'Appennino umbro-marchigiano tra il pedappennino umbro e la costa adriatica.  
572 Boll. Soc. Geol. It. 118, 125-139 (in Italian).
- 573 Cavazza, W., Roure, F., Ziegler, P.A., 2004. The Mediterranean area and the surrounding regions:  
574 active processes, remnants of former Tethyan oceans and related thrust belts, in: Cavazza, W.,  
575 Roure, F., Spakman, W., Stampf, G.M., Ziegler, P.A. (Eds.), The TRANSMED Atlas. The  
576 Mediterranean Region from crust to mantle. Springer, Berlin, pp. 1–29.
- 577 Centamore, E., Deiana, G., Micarelli, A., Potetti, M., 1986. Il Trias-Paleogene delle Marche, in:  
578 Centamore, E., Deiana, G. (Eds.), La Geologia delle Marche. Studi Geol. Camerti, Volume  
579 Speciale, pp. 9-27 (in Italian).
- 580 Centamore, E., Cantalamessa, G., Micarelli, A., Potetti, M., Berti, D., Bigi, S., Morelli, C., Ridolfi,  
581 M., 1991. Stratigrafia ed analisi di facies dei depositi del Miocene e del Pliocene inferiore  
582 dell'avanfossa marchigiano-abruzzese e delle avanfosse limitrofe. Studi Geol. Camerti, Vol. Spec.  
583 1991/2, 125-132 (in Italian).
- 584 Ciancimino, A., Lanzo, G., Alleanza, G.A., Amoroso, S., Bardotti, R., Biondi, G., Cascone, E.,  
585 Castelli, F., Di Giulio, A., D'Onofrio, A., Foti, S., Lentini, V., Madiari, C., Vessia, G., 2020.  
586 Dynamic characterization of fine-grained soils in Central Italy by laboratory testing.  
587 Bull.Earthq.Eng. 18, 5503-5531. <https://doi.org/10.1007/s10518-019-00611-6>.
- 588 Coltorti, M., Pieruccini, P., 1999. A late Lower Pliocene planation surface across the Italian  
589 Peninsula: a key tool in neotectonic studies. Journal of Geodynamics 29, 323-328.  
590 [https://doi.org/10.1016/S0264-3707\(99\)00049-6](https://doi.org/10.1016/S0264-3707(99)00049-6).
- 591 Cosentino, D., Cipollari, P., Marsili, P., Scrocca, D., 2010. Geology of the central Apennines: a  
592 regional review, in: Beltrando, M., Peccerillo, A., Mattei, M., Conticelli, S., Doglioni, C. (Eds.),  
593 Journal of the Virtual Explorer, 36, paper 11. doi:10.3809/jvirtex.2009.00223.
- 594 CTMS (Commissione tecnica per la Microzonazione sismica), 2018. Standard di Rappresentazione  
595 ed archiviazione informatica, versione 4.1.1, Dept.of Civil Protection, Rome (in Italian), available  
596 on the website: <https://www.centromicrozonazioneisismica.it/it/download/send/26-standardms-41/71-standardms-4-1>.  
597
- 598 DB-SM. Portale cartografico della Microzonazione Sismica e della Condizione Limite per  
599 l'Emergenza, <https://www.webms.it/servizi/viewer.php>; 2019 [accessed, March 2020].
- 600 EN 1998-1, 2004. Eurocode 8: Design of structures for earthquake resistance. Part 1: General rules,  
601 seismic actions and rules for buildings, Brussels.
- 602 Faccioli, E. (Ed.), 1986. Elementi per una guida alle indagini di microzonazione sismica, Consiglio  
603 Nazione delle Ricerche, Rome (in Italian).
- 604 Foti, S., Parolai, S., Albarello, D., Picozzi, M., 2011. Application of surface wave methods for seismic  
605 site characterization. Surv.Geophys. 32, 6, 777-825. DOI 10.1007/s10712-011-9134-2.
- 606 Foti, S., Hollender, F., Garofalo, F., Albarello, D., Asten, M., Bard, P.Y., Comina, C., Cornou, C.,  
607 Cox, B., Di Giulio, G., Forbriger, T., Hayashi, K., Lunedei, E., Martin, A., Mercerat, D.,  
608 Ohrnberger, M., Poggi, V., Renalier, F., Sicilia, D., Socco, V., 2017. Guidelines for the good



- 609 practice of surface wave analysis: a product of the InterPACIFIC project. *Bull.Earthq.Eng.*  
610 16, 2367–2420. <https://doi.org/10.1007/s10518-017-0206-7>.
- 611 Galli, P., Castenetto, S., Peronace, E., 2017. The macroseismic intensity distribution of the 30 October  
612 2016 earthquake in central Italy (Mw 6.6): seismotectonic implications. *Tectonics* 36, 2179-2191.  
613 <https://doi.org/10.1002/2017TC004583>.
- 614 García-Jerez, A., Piña-Flores, J., Sánchez-Sesma, F.J., Luzón, F., Perton, M., 2016. A computer code  
615 for forward computation and inversion of the H/V spectral ratio under the diffuse field assumption.  
616 *Computers & Geosciences* 97, 67-78. <https://doi.org/10.1016/j.cageo.2016.06.016>.
- 617 IAEA, 2016. Seismic hazard assessment in site evaluation for nuclear installations: ground motion  
618 prediction equations and site response, IAEA-TECDOC-1796, Wien.
- 619 Khan, S., Waseem, M., Khan, M.A., Hussain Z., Ahmed W., Khliq A.H., Umair N.S., Hissain M.L.,  
620 2020. Microzonation map of the Abbottabad basin and immediate surroundings. *J Seismol* 24,  
621 165–181 (2020). <https://doi.org/10.1007/s10950-019-09895-2>
- 622 Kottke, A.R. and Rathje E.M.. 2008. "Technical manual for Strata." Report No.: 2008/10. Pacific  
623 Earthquake Engineering Research Center, University of California, Berkeley.
- 624 Kramer, S.L., 1996. *Geotechnical Earthquake Engineering*, Prentice Hall, New Jersey, USA.
- 625 Lachet, C., Bard, P.Y., 1994. Numerical and theoretical investigations on the possibilities and  
626 limitations of Nakamura's technique. *J Geophys Earth* 42, 377-397.  
627 <https://doi.org/10.4294/jpe1952.42.377>.
- 628 Mase, L.Z., Sugianto, N. & Refrizon, 2021. Seismic hazard microzonation of Bengkulu City,  
629 Indonesia. *Geoenviron Disasters* 8, 5. <https://doi.org/10.1186/s40677-021-00178-y> Medvedev,  
630 S.V., 1965. *Engineering Seismology*, Israel Program fo Scientific Translations Ltd., Jerusalem.
- 631 Molnar S., Assaf J., Sirohey A., Adhikari S.R., 2020. Overview of local site effects and seismic  
632 microzonation mapping in Metropolitan Vancouver, British Columbia, Canada, *Eng. Geol.*, 270,  
633 105568, <https://doi.org/10.1016/j.enggeo.2020.105568>.
- 634 Mori, F., Gaudiosi, I., Tarquini, E., Brammerini, F., Castenetto, S., Naso, G., Spina, D., 2020. HSM: a  
635 synthetic damage- constrained seismic hazard parameter. *Bull.Earthq.Eng.* 18, 5631-5654.  
636 <https://doi.org/10.1007/s10518-019-00677-2>.
- 637 Moscatelli, M., Albarello, D., Scarascia Mugnozza, G., Dolce, M., 2020. The Italian approach to  
638 seismic microzonation. *Bull.Earthq.Eng.* 18, 5425–5440. <https://doi.org/10.1007/s10518-020-00856-6>.
- 640 NTC, 2018. *Norme Tecniche per le Costruzioni*. Decreto del Ministero delle Infrastrutture, GU serie  
641 generale n.42, 20-02-2018 – Suppl. Ordinario n.8
- 642 Okada, H., 2003. *The microtremor survey method*, Geophysical Monograph Series, 12, Society of  
643 Exploration Geophysicists. <https://doi.org/10.1190/1.9781560801740>.
- 644 Pagliaroli, A., Pergalani, F., Ciancimino, A., Chiaradonna, A., Compagnoni, M., De Silva, F., Foti,  
645 S., Giallini, S., Lanzo, G., Lombardi, F., Luzi, L., Macerola, L., Nocentini, M., Pizzi, A., Tallini,  
646 M., Teramo, C., 2020. Site response analyses for complex geological and morphological  
647 conditions: relevant case-histories from 3rd level seismic microzonation in Central Italy.  
648 *Bull.Earthq.Eng.* 18, 5741–5777. <https://doi.org/10.1007/s10518-019-00610-7>.

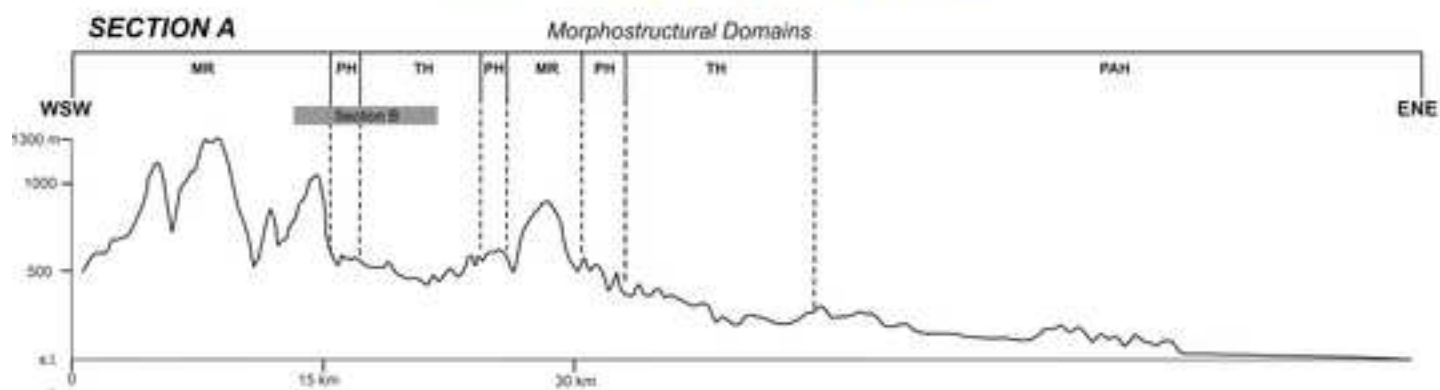
- 649 Paolucci, R., 2002. Amplification of earthquake ground motion by steep topographic irregularities.  
650 Earthquake Engineering and Structural Dynamics 31, 1831-1853. <https://doi.org/10.1002/eqe.192>.
- 651 Paolucci, E., Tanzini, A., Peruzzi, G., Albarello, D., Tiberi, P., 2020. Empirical testing of a simplified  
652 approach for the estimation of 1D lithostratigraphical amplification factor. Bull.Earthq.Eng. 18,  
653 1285–1301. <https://doi.org/10.1007/s10518-019-00772-4>.
- 654 Park, C.B., 2011. Imaging dispersion of MASW data - full vs. selective offset scheme. Journal of  
655 Environmental and Engineering Geophysics 16, 1, 13-23. <https://doi.org/10.2113/JEEG16.1.13>.
- 656 Peruzzi, G., Albarello, D., Baglione, M., D'Intinosante, V., Fabbroni, P., Pileggi, D., 2016. Assessing  
657 1D seismic response in microzoning studies in Italy. Bull.Earthq.Eng. 14, 373-389.  
658 <https://doi.org/10.1007/s10518-015-9841-z>.
- 659 Régnier J., Bertrand E., Cadet H., 2020. Repeatable process for seismic microzonation using 1-D site-  
660 specific response spectra assessment approaches. Application to the city of Nice, France, Eng.  
661 Geol., 270, 105569, <https://doi.org/10.1016/j.enggeo.2020.105569>.
- 662 Salsabili, M., Saeidi, A., Rouleau, A., Nastev N., , 2021. Seismic microzonation of a region with  
663 complex surficial geology based on different site classification approaches. Geoenviron. Disasters  
664 8, 27 (2021). <https://doi.org/10.1186/s40677-021-00198-8>
- 665 Thitimakorn T., 2019. Seismic microzonation maps of Phrae city, Northern Thailand, Geomatics,  
666 Natural Hazards and Risk, 10:1, 2276-2290, DOI: 10.1080/19475705.2019.1693705
- 667 Various Authors, 2011. Contributi per l'aggiornamento degli "Indirizzi e criteri per la  
668 microzonazione sismica", in: Ingegneria Sismica, 28, 2, Patron editore, Bologna, Italy (in Italian),  
669 [http://www.protezionecivile.gov.it/resources/cms/documents/aggiornamento\\_indirizzi\\_microzonazione\\_sismica.pdf](http://www.protezionecivile.gov.it/resources/cms/documents/aggiornamento_indirizzi_microzonazione_sismica.pdf).
- 671 WGSM (Working Group on Seismic Microzoning), 2008. Indirizzi e criteri per la microzonazione  
672 sismica, Conferenza delle Regioni e delle Province autonome – Dipartimento della Protezione  
673 Civile, Rome, 3 vol. and DVD (in Italian),  
674 [http://www.protezionecivile.gov.it/jcms/it/view\\_pub.wp?contentId=PUB1137](http://www.protezionecivile.gov.it/jcms/it/view_pub.wp?contentId=PUB1137), English version at  
675 [http://www.protezionecivile.gov.it/httpdocs/cms/attach\\_extra/GuidelinesForSeismicMicrozonation.pdf?](http://www.protezionecivile.gov.it/httpdocs/cms/attach_extra/GuidelinesForSeismicMicrozonation.pdf?)  
676
- 677 WGSMLA (Working Group on Seismic Microzoning the L'Aquila Area), 2010. Microzonazione  
678 sismica per la ricostruzione dell'area aquilana, Regione Abruzzo, Dipartimento della Protezione  
679 Civile, 3 vols and DVD, 796 pp. (in Italian),  
680 [http://www.protezionecivile.gov.it/jcms/it/view\\_pub.wp?contentId=PUB25330](http://www.protezionecivile.gov.it/jcms/it/view_pub.wp?contentId=PUB25330).



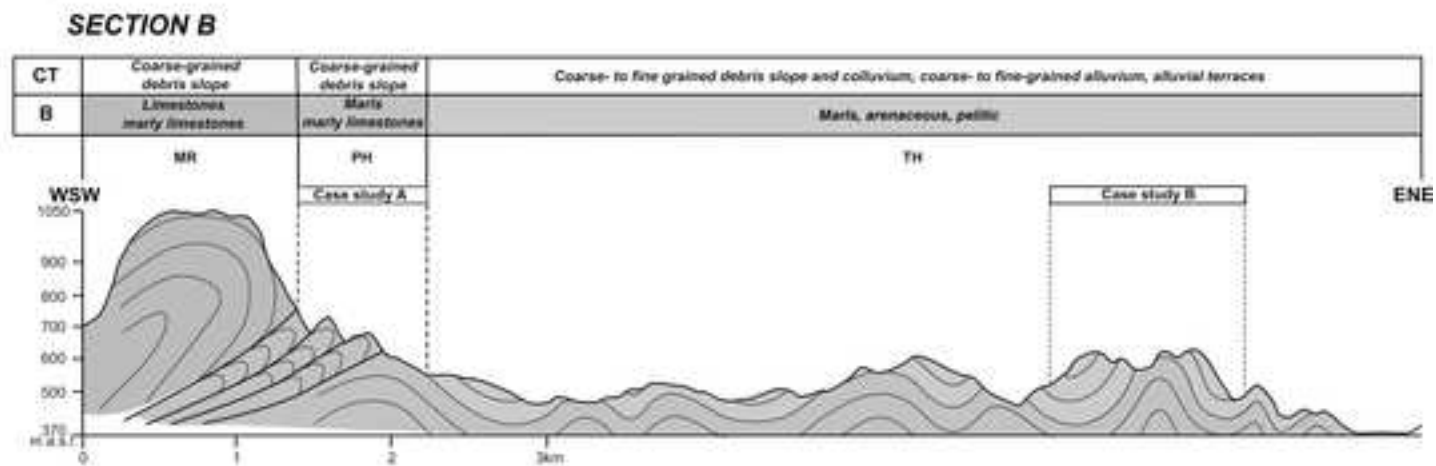




a



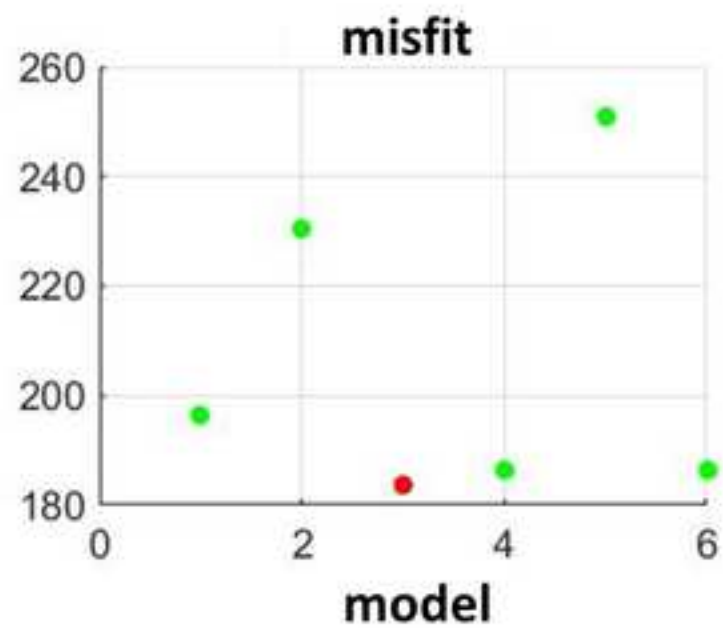
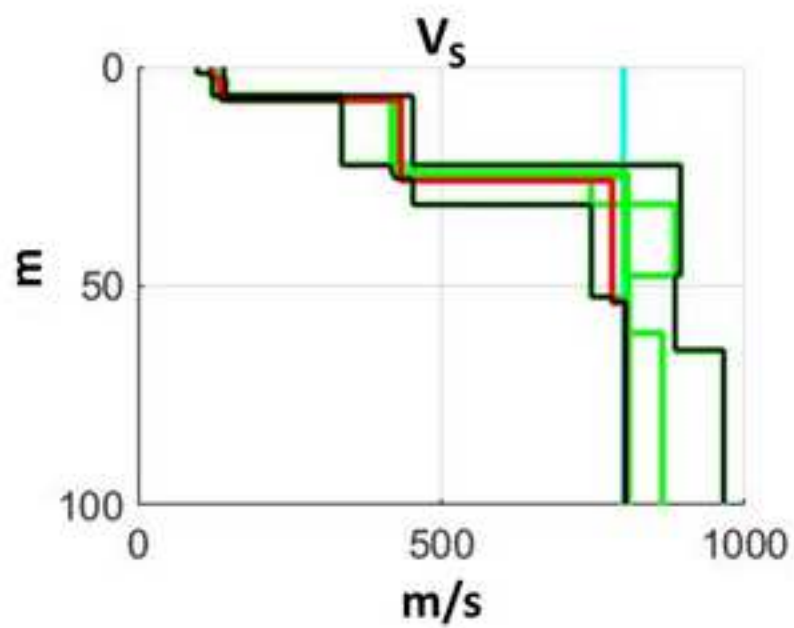
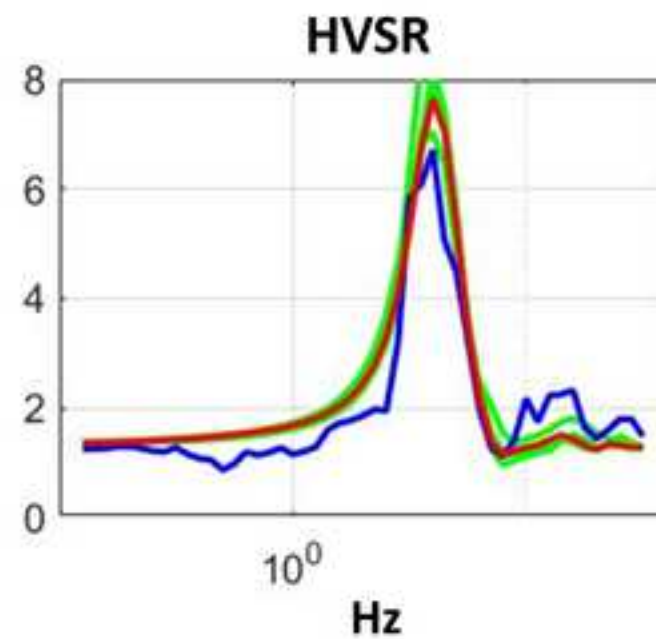
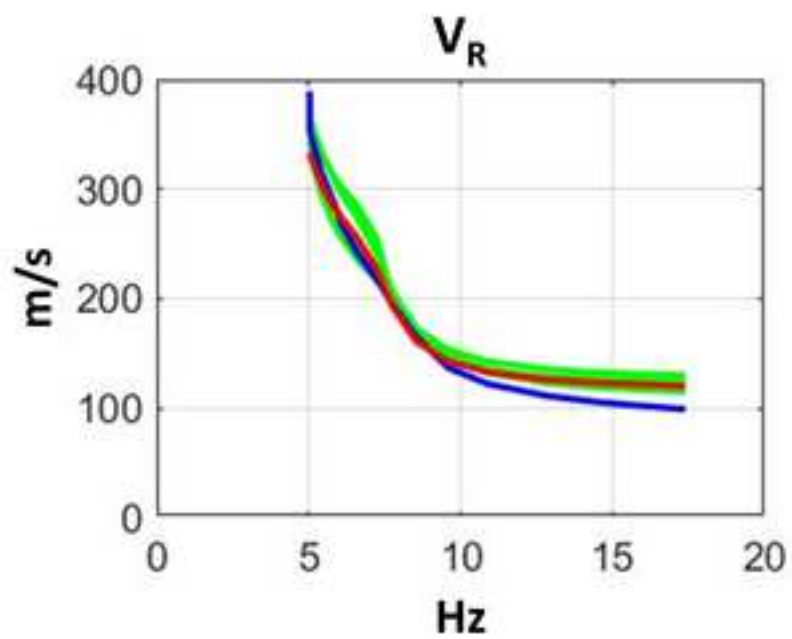
b



c

SE - S.ERASMO						AR - ARNANO											
log id	Min (m)	Max (m)	B/CT	gt code	Description	log id	Min (m)	Max (m)	B/CT	gt code	Description	log id	Min (m)	Max (m)	B/CT	gt code	Description
1	2	5	CT	ML	Unsorted low plasticity silts, clays and sands	2	5	25	CT	GP	Angular to subangular unsorted calcareous debris-slope, weakly to strongly cemented	1	5	20	CT	GP	Angular to subangular unsorted calcareous debris-slope, weakly to strongly cemented
	30	140	B	COS	Marls and clays (SCH Fm)												
	10	70	B	ALS	Marly limestones (BIS Fm)												
CA - CALCINA																	
log id	Min (m)	Max (m)	B/CT	gt code	Description	log id	Min (m)	Max (m)	B/CT	gt code	Description	log id	Min (m)	Max (m)	B/CT	gt code	Description
1	70	100	B	ALS	Marly limestones (BIS Fm)	2	5	25	CT	GP	Angular to subangular unsorted calcareous debris-slope, weakly to strongly cemented	3	5	15	CT	GP	Angular to subangular, loose, unsorted calcareous debris
	5	30		ALS	Marly limestones (BIS Fm)		B	ALS	Marly limestones (BIS Fm)								

SM - S. MARCELLO																					
log id	Min (m)	Max (m)	B/CT	gt code	Description	log id	Min (m)	Max (m)	B/CT	gt code	Description	log id	Min (m)	Max (m)	B/CT	gt code	Description				
1	3	10	CT	ML	Holocene fine-grained unsorted eluvial and colluvial deposits	2					Marls and clays (SCH Fm)	3	3	10	CT	ML	Holocene fine-grained unsorted eluvial and colluvial deposits				
	3	15	CT	GM	Pleistocene alluvial packed unsorted gravels and sands																
				B	COS		Marls and clays (SCH Fm)			B			COS	Marls and clays (SCH Fm)							
SN - SENTINO						SS - S. SILVESTRO															
log id	Min (m)	Max (m)	B/CT	gt code	Description	log id	Min (m)	Max (m)	B/CT	gt code	Description	log id	Min (m)	Max (m)	B/CT	gt code	Description				
1	3	50	B	GRS	Arenaceous lithofacies (FCId Fm)	1					Marls and clays (SCH Fm)	2					Marls and clays (SCH Fm)				
	15	15	B	COS	Pelitic-arenaceous lithofacies (FCId Fm)										3	100		B	GRS	Arenaceous lithofacies (FCId Fm)	
	3	30	B	GRS	Arenaceous lithofacies (FCId Fm)				B	COS											
				B	COS		Marls and clays (SCH Fm)												B	COS	Marls and clays (SCH Fm)









## PEDEMOUNTAIN HILLS

## TERRIGENOUS HILLS

